Research on PMSM Position Sensorless Control with EKF(Extended Kalman Filter)

平成 29 年度
三重大学大学院工学研究科　博士前期課程
電気電子工学専攻　電気システム工学講座

WANG YANKAI

三重大学大学院　工学研究科

Contents

Contents

Chapter1 Abstract

1.1 Background of the research

1.1.1 Brief classification of motor[1][2][3][4]

Motor is a kind of electrical machine which converts electrical energy into mechanical one. With recent development and improvement, the structure of motor is usually made up of rotor part and stator part. By classification of driving strategy. There are two kinds of motor, DC motor and AC motor.

(1). DC motor: The driving current of DC motor is direct current. The motor has a commutator. It causes sparks when DC motor runs with large current. To avoid this problem, brushless DC motor[1] has been invented. But both of them(DC motor and brushless DC motor) require a complicated DC power supply system, which causes power losses when electricity power is alternated.

(2). AC motor: The driving signal of AC motor is sinusoidal current. This kind of motor usually has three-phase currents. Each phase current is apart from each other by 120 degrees in space. In AC motors, there are two popular ones, induction motor and synchronous motor. In induction motor, rotor speed lags behind stator speed. This is named slip, and slip is the reason why induction motor cannot achieve high efficiency. Synchronous can be divided by rotor structure as wound rotor synchronous motor and PMSM(permanent magnet synchronous motor). The paper targets PMSM as the controlled plant. The structure of PMSM is introduced in detail within Chapter 2. The mentioned motor classification is shown in Fig.1.1

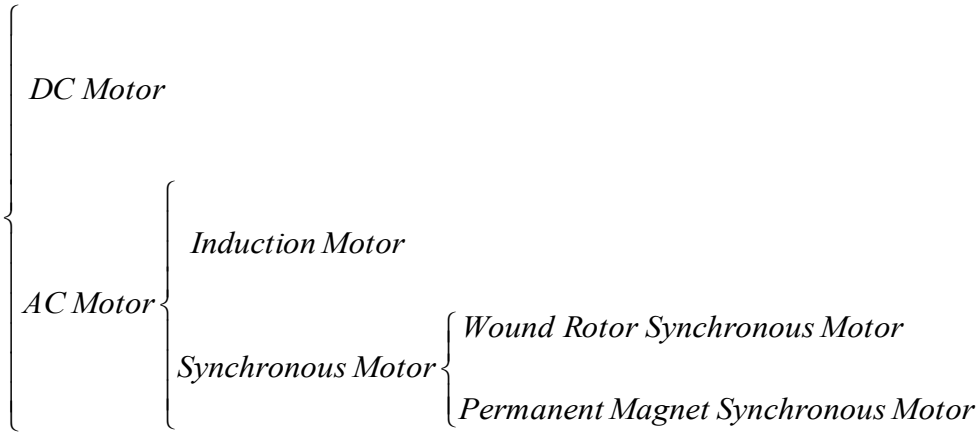

Fig.1.1 Brief motor classification

1.1.2 PMSM speed control strategy

PMSM speed control system is complicated. Compared with brush DC motor speed control system, it is more difficult for PMSM to achieve high accuracy, stability and fast response. Nowadays, researchers and engineers are focusing on improving these characteristics for PMSM speed control system. There are mainly three achievements.

(1). VVVF(Variable voltage variable frequency) Control[5]

VVVF control strategy is an early speed control method for AC motors, including PMSM. It was firstly proposed to achieve AC motor speed control because it is a constant when supply voltage divided by motor frequency, if the flux is not altered.

(2). DTC(Direct Torque Control)[6]

DTC control strategy is a loop control method for AC motors. It was first proposed by Dr. Depenbrock in 1985. This kind of control strategy get electrical driving torque by calculating stator flux.

(3). FOC(Field Oriented Control)[7][8]

FOC control strategy was proposed by Siemens engineer in 1970s. From that time, vector control for AC motor has been applied into motor speed control field. With Park and Clerk transformation, this control strategy has been greatly imporved. In this paper, this control strategy has been applied. And will be introduced in Chapter 2.

1.1.3 PMSM position sensorless speed control strategy

Position sensorless speed control strategy for PMSM reduces the whole system cost and makes the system be possible to work in high dust environment. There are a lot of methods to achieve the sensorless control. The methods are classified according to the motor speed.

(1). High-speed position sensorless method[9][10][11]

High-speed position sensorless control method usually uses voltage and current which contain Back-EMF signals to estimate the position and speed information. By these estimations, position sensorless control is achieved in high-speed region.

(2). Low-speed position sensorless method[12][13]

Low-speed position sensorless control method usually injects small amplitude high frequency signal in d-axis. If the motor has salient pole, a large induced voltage happens. With this saliency of PMSM, it can achieve low-speed position sensorless control.

1.2 Aims of the study

This study aims at IPMSM position sensorless control in low speed range with EKF(Extended Kalman Filter). As our former method cannot achieve low-speed range position sensorless control. EKF can solve the problem above to some extend. To achieve better system characteristics, a d-axis current random signal injection method with EKF is proposed, which makes EKF be able to achieve better IPMSM position sensorless control in low speed-range.

1.3 Comparison with former study

The former method is EEMF Observer. This method can achieve IPMSM position sensorless control above 300rpm. 300rpm is defined as the boundary between high and low-speed region. By using d-axis current random signal injection method with EKF, IPMSM can achieve low-speed range position sensorless control. The lowest controlled speed is 0 rpm. To improve robustness to load torque, noise balanced matrix Q of EKF is compensated.

1.4 Composition of the paper

This paper is made up of the following 7 parts.

Chapter 1 is the abstract. It includes background and aims of the study and comparison with former one.

Chapter 2 introduces about basic characteristics of PMSM, which includes PMSM construction, mathematics dynamics and FOC strategy.

Chapter 3 discusses about EEMF Observer for PMSM position sensorless control, which is the former study method. After analyzing, the weakness of EEMF Observer is pointed out.

Chapter 4 introduces EKF(Extended Kalman Filter) for IPMSM. Addtionally, d-axis current random signal injection method with EKF will be discussed in this part.

Chapter 5 shows simulation results to prove the aims of this study.

Chapter 6 is the conclusions according to the discussion and simulation results. Then, the future plan is given.

Chapter2. Basic characteristics of Permanent Magnet Synchronous Motor (PMSM) [14][15][16][17]

2.1 Coordinate transformation

Because of PMSM nonlinearity, and strong coupling, it is difficult to control PMSM in ordinary space coordinate axis. For this reason, an appropriate coordinate axis is required to analyze PMSM.

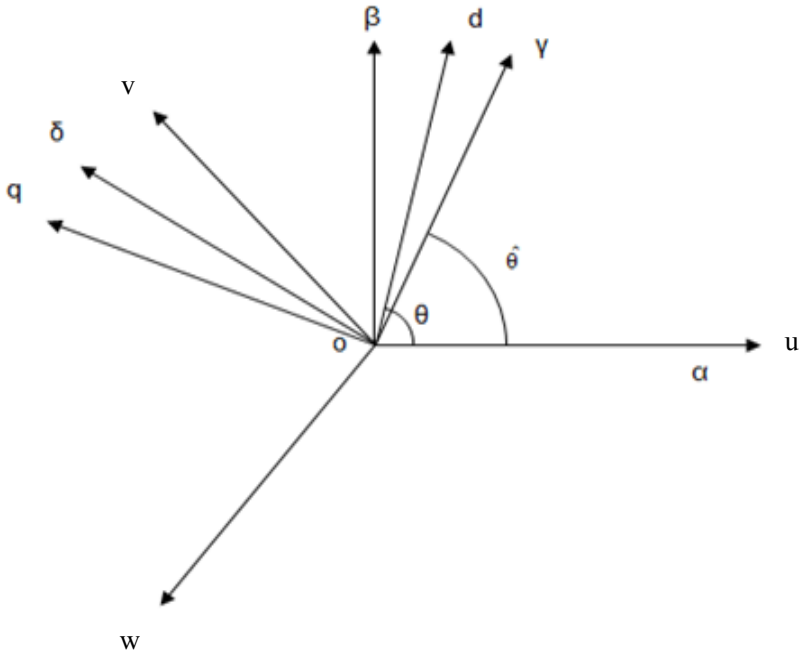

Fig. 2.1 Relationships between coordinate axis respectively

In Fig. 2.1, uvw axis is ordinary stationary three coordinate axis. $\alpha\beta$ axis is stationary two coordinate axis, which is transformed from uvw axis by Clerk transformation. dq axis is rotated two coordinate axis, which is rotated from $\alpha\beta$ axis by Park transformation. $\gamma\delta$ is the estimated axis of dq . Clerk and Park transformations are defined as follows:

(1). Clerk transformation

By the space relationships between uvw and $\alpha\beta$ axis, it is easy to get the relationships:

$$\begin{bmatrix} f_\alpha \\ f_\beta \\ f_0 \end{bmatrix} = K \begin{bmatrix} 1 & -\frac{1}{2} & -\frac{1}{2} \\ 0 & \frac{\sqrt{3}}{2} & -\frac{\sqrt{3}}{2} \\ m & m & m \end{bmatrix} \begin{bmatrix} f_u \\ f_v \\ f_w \end{bmatrix} = T_{3s-2s} \begin{bmatrix} f_u \\ f_v \\ f_w \end{bmatrix} \tag{2.1}$$

Following is the calculation methods for coefficient K and m. Let us set T_{3s-2s} in eq.(2.1) as matrix [T], ordinary stationary three coordinate axis motor equation can be simplified as:

$$[v] = [z][i] + [e] \tag{2.2}$$

$$[T][v] = [T][z][T]^{-1}[T][i] + [T][e] \tag{2.3}$$

By eq.(2.3), eq.(2.2) can be assumed as:

$$[T][v] = [v'],\ [T][i] = [i'],\ [T][z][T]^{-1}[i'] = [z'][i'],\ [T][e] = [e'] \tag{2.4}$$

It can get:

$$[v'] = [z'][i'] + [e'] \tag{2.5}$$

To satisfy a condition that power is not changed by coordinate transformation, the combining eq.(2.2) to eq.(2.5), eq.(2.6) is given.

$$[\mathrm{v}]^{\mathrm{T}}[i] = [v']^T[i'] = [[T][v]]^T[T][i] = [v]^T[T]^T[T][i] \tag{2.6}$$

According to the matrix basic characteristics, and consider eq.(2.6), eq.(2.7) should be satisfied.

$$[T]^{-1}[T] = [T]^T[T] = [I] \tag{2.7}$$

As a result, eq.(2.8) is given as constraint condition.

$$[T]^{-1} = [T]^T \tag{2.8}$$

From eq.(2.8),

$$T_{3s-2s} = \sqrt{\frac{2}{3}} \begin{bmatrix} 1 & -\frac{1}{2} & -\frac{1}{2} \\ 0 & \frac{\sqrt{3}}{2} & -\frac{\sqrt{3}}{2} \\ \frac{1}{\sqrt{2}} & \frac{1}{\sqrt{2}} & \frac{1}{\sqrt{2}} \end{bmatrix}$$

Usually, the third line of eq.(2.9) can be ignored. It can be written as:

$$T_{3s-2s} = \sqrt{\frac{2}{3}}\begin{bmatrix} 1 & -\frac{1}{2} & -\frac{1}{2} \\ 0 & \frac{\sqrt{3}}{2} & -\frac{\sqrt{3}}{2} \end{bmatrix} \tag{2.10}$$

The transport matrix of eq.(2.10) can achieve stationary two coordinate axis to stationary three coordinate axis transformation. It is shown in eq.(2.11)

$$\begin{bmatrix} f_u \\ f_v \\ f_w \end{bmatrix} = \sqrt{\frac{2}{3}}\begin{bmatrix} 1 & 0 \\ -\frac{1}{2} & \frac{\sqrt{3}}{2} \\ -\frac{1}{2} & -\frac{\sqrt{3}}{2} \end{bmatrix}\begin{bmatrix} f_\alpha \\ f_\beta \end{bmatrix} = T_{3s-2s}^{-1}\begin{bmatrix} f_\alpha \\ f_\beta \end{bmatrix} \tag{2.11}$$

Eq.(2.10) and eq.(2.11) are Clerk transformation and inverse Clerk transformation. By transfer matrix T_{3s-2s} and T_{3s-2r}^{-1}, stationary two coordinate axis to stationary three coordinate axis transformation can be achieved.

(2). Park transformation

From relationships between $\alpha\beta$ axis and dq axis in Fig.2.1, their mathematics relationships is shown as follows.

$$\begin{bmatrix} f_d \\ f_q \\ f_0 \end{bmatrix} = \begin{bmatrix} \cos\theta & \sin\theta & 0 \\ -\sin\theta & \cos\theta & 0 \\ 0 & 0 & 1 \end{bmatrix}\begin{bmatrix} f_\alpha \\ f_\beta \\ f_0 \end{bmatrix} = T_{2s-2r}\begin{bmatrix} f_\alpha \\ f_\beta \\ f_0 \end{bmatrix} \tag{2.12}$$

$$\begin{bmatrix} f_\alpha \\ f_\beta \\ f_0 \end{bmatrix} = \begin{bmatrix} \cos\theta & -\sin\theta & 0 \\ \sin\theta & \cos\theta & 0 \\ 0 & 0 & 1 \end{bmatrix}\begin{bmatrix} f_d \\ f_q \\ f_0 \end{bmatrix} = T_{2s-2r}^{-1}\begin{bmatrix} f_d \\ f_q \\ f_0 \end{bmatrix} \tag{2.13}$$

2.2 Models of PMSM

2.2.1 Construction

PMSM is a kind of electric motor that permanent magnets are installed on the rotor to generate magnetic fields. In this way, it can avoid commutator brush problem in DC motor. There are two kinds of rotor structure of PMSM in Fig.2.2. The left one is interior permanent magnet synchronous motor(IPMSM), and right one is surface-mounted permanent magnet synchronous motor(SPMSM). In IPMSM, the magnetic resistances are different from each other on dq axis in mathematics voltage models, while in SPMSM, the magnetic resistances are the same.

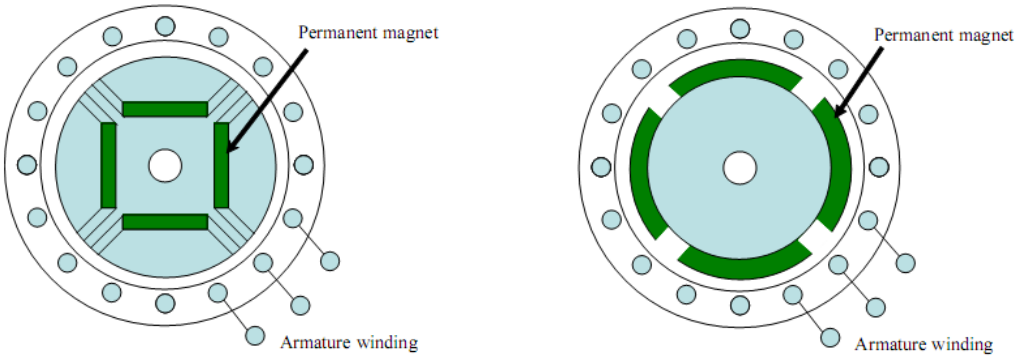

(a)IPMSM (b)SPMSM

Fig.2.2 Rotor structure of PMSM

2.2.2 Electronics mathematics models of PMSM

（1）*u-v-w* axis mathematics models

Fig.2.3 is the 3 phases PMSM equivalent circuit. The voltage, current and impedance equivalent equation is shown as eq.(2.14)

$$\begin{bmatrix} v_u \\ v_v \\ v_w \end{bmatrix} = \begin{bmatrix} R_a + pL_a^{'} & -\frac{1}{2}pM_a^{'} & -\frac{1}{2}pM_a^{'} \\ -\frac{1}{2}pM_a^{'} & R_a + pL_a^{'} & -\frac{1}{2}pM_a^{'} \\ -\frac{1}{2}pM_a^{'} & -\frac{1}{2}pM_a^{'} & R_a + pL_a^{'} \end{bmatrix} \begin{bmatrix} i_u \\ i_v \\ i_w \end{bmatrix} + \begin{bmatrix} e_u \\ e_v \\ e_w \end{bmatrix} \tag{2.14}$$

Here, v_u, v_v, v_w are phase voltages, i_u, i_v, i_w are *uvw* phase stator currents, e_u, e_v, e_w are Back-electromotive forces, R_a is winding resistor, L_a' is the winding inductance of motor, M_a' is mutual inductance of winding, $p(=d/dt)$ means differential symbol.

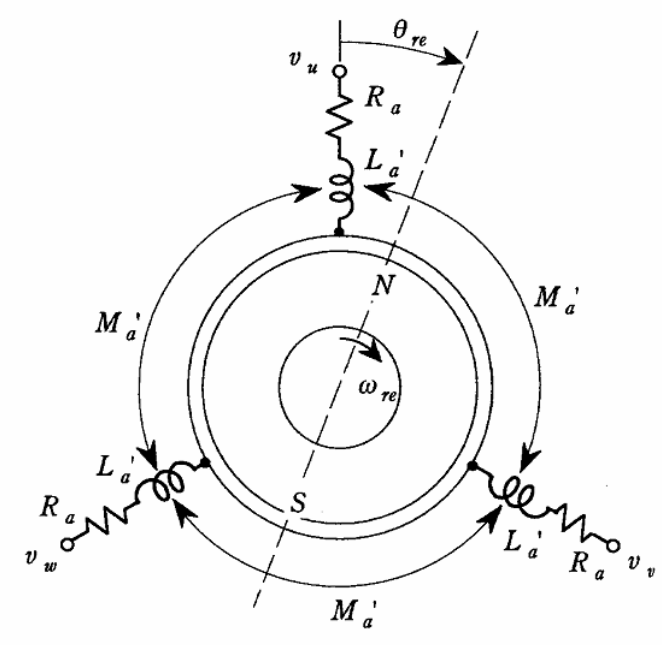

Fig. 2.3 Three-phase PMSM equivalent circuit

Let us define peak value of *uvw* phases rotor flux ϕ_{fu} , ϕ_{fv} , ϕ_{fw} as $\phi_f^{'}$. They are caused by electromotive forces e_u, e_v, e_w. Rotor flux is shown as:

$$\begin{aligned}\phi_{fu} &= \phi_f^{'}\cos\theta_{re}\\ \phi_{fv} &= \phi_f^{'}\cos\left(\theta_{re}-\frac{2\pi}{3}\right)\\ \phi_{fw} &= \phi_f^{'}\cos\left(\theta_{re}+\frac{2\pi}{3}\right)\end{aligned} \tag{2.15}$$

θ_{re} is the rotor electrical angle, which is based on *u* phase axis. ω_{re} is the permanent magnet rotating speed. It is defined as rotor electrical speed,

$$\theta_{re} = \int \omega_{re} dt \tag{2.16}$$

Which should be pointed out is that PMSM rotating speed (Mechanical speed) ω_{rm} has the relationship with pole pairs p.

$$\omega_{rm} = \omega_{re} / p \tag{2.17}$$

At this time, electromotive forces e_u, e_v, e_w can be defined as:

$$\begin{aligned}e_u &= p\phi_{fu} = -\omega_{re}\phi_f^{'}\sin\theta_{re}\\ e_v &= p\phi_{fv} = -\omega_{re}\phi_f^{'}\sin\left(\theta_{re}-\frac{2\pi}{3}\right)\\ e_w &= p\phi_{fw} = -\omega_{re}\phi_f^{'}\sin\left(\theta_{re}+\frac{2\pi}{3}\right)\end{aligned} \tag{2.18}$$

The leakage inductance of each winding is defined as l_a . It has the relationship with winding inductance L_a and mutual inductance $M_a^{'}$ as:

$$L_a = l_a + M_a^{'} \tag{2.19}$$

（2） $\alpha\beta$ axis voltage equation

By three to two phase coordinate stationary transformation, $\alpha\beta$ axis PMSM models is given.

The characteristics of transfer matrix [c] in Fig.2.4 is $v_u+v_v+v_w=0$, $i_u+i_v+i_w=0$.

$$[c]=\sqrt{\frac{2}{3}}\begin{bmatrix}1 & -\frac{1}{2} & -\frac{1}{2}\\ 0 & \frac{\sqrt{3}}{2} & -\frac{\sqrt{3}}{2}\end{bmatrix} \tag{2.20}$$

By using eq. (2.20) into The voltage, current and impedance equivalent equation eq.(2.14),

$$\begin{bmatrix}v_\alpha\\ v_\beta\end{bmatrix}=R_\alpha\begin{bmatrix}i_\alpha\\ i_\beta\end{bmatrix}+\begin{bmatrix}pL_d & \omega_{re}(L_d-L_q)\\ -\omega_{re}(L_d-L_q) & pL_d\end{bmatrix}\begin{bmatrix}i_\alpha\\ i_\beta\end{bmatrix}+\begin{bmatrix}e_\alpha\\ e_\beta\end{bmatrix} \tag{2.21}$$

v_α, v_β ------ the stator voltages on α , β axis ;

i_α, i_β ------ the stator currents on α , β axis ;

P ------ differential coefficient;

L_d ------ d-axis inductance;

L_q ------ q-axis inductance;

e_α, e_β ------ electromotive force signals on α , β axis;

$\dot{i}_q$ ------ q-axis current differential coefficient.

Electromotive force signals e_α, e_β can be written as:

$$\begin{bmatrix}e_\alpha\\ e_\beta\end{bmatrix}=\left\{(L_d-L_q)\left(\omega_{re}i_d-\dot{i}_q\right)+\omega_{re}\phi_f\right\}\begin{bmatrix}-\sin\theta_{re}\\ \cos\theta_{re}\end{bmatrix} \tag{2.22}$$

Here, ϕ_f has the relationship with ϕ_f' in eq. (2.15) as

$$\phi_f=\sqrt{\frac{3}{2}}\phi_f' \tag{2.23}$$

As a result, e_α , e_β are represented as eq.(2.24)

$$\begin{aligned}e_\alpha &= p\phi_{f\alpha}=-\omega_{re}\phi_f\sin\theta_{re}\\ e_\beta &= p\phi_{f\beta}=-\omega_{re}\phi_f\cos\theta_{re}\end{aligned} \tag{2.24}$$

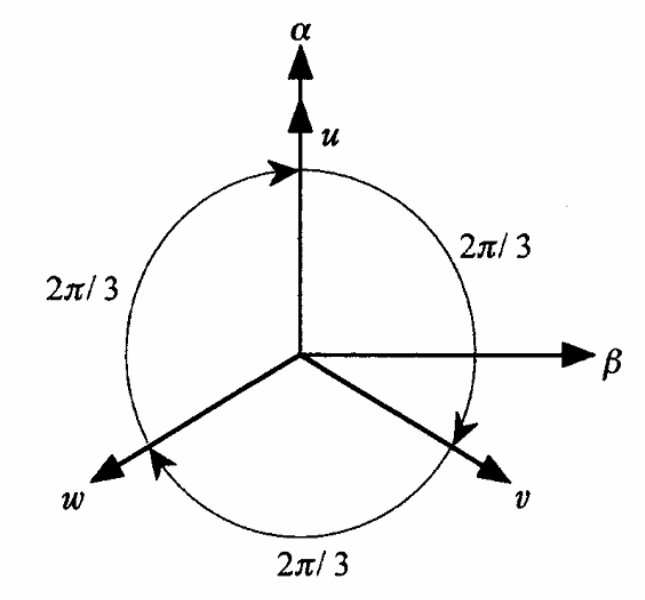

Fig.2.4　Relationships between ordinary stationary 3 coordinate（*u* -*v*-*w*）and stationary 2 coordinate（$\alpha-\beta$）

（3） *d* - *q* axis mathematics models

Motor is a machine that has stator part and rotor part. The transformation from stationary two coordinate to rotated two coordinate is called *d*-*q* transformation. As a result, there is *d*-*q* axis. *q* axis is ahead of *d* axis in phase by π/2.

In PMSM, *d* axis represents the motor stator flux direction, while q axis represents the motor torque axis. There is *d*-*q* space axis.

Stationary two coordinate axis （$\alpha-\beta$） to rotated two coordinate *d*-*q* matrix matrix [*c*].

$$[c]=\begin{bmatrix}\cos\theta_{re} & \sin\theta_{re}\\ -\sin\theta_{re} & \cos\theta_{re}\end{bmatrix} \tag{2.25}$$

This matrix is calculated by trigonometric function from Fig. 2.5.

With eq.(2.12), *d*-*q* axis voltage equation can be shown as:

$$\begin{bmatrix}v_d\\ v_q\end{bmatrix}=\begin{bmatrix}R_\alpha+pL_d & -\omega_{re}L_q\\ \omega_{re}L_q & R_\alpha+pL_d\end{bmatrix}\begin{bmatrix}i_d\\ i_q\end{bmatrix}+\begin{bmatrix}0\\ (L_d-L_q)(\omega_{re}i_d-\dot{i}_q)+\omega_{re}\phi_f\end{bmatrix} \tag{2.26}$$

The 2nd section in the right side of eq.(2.26) is the electromotive force terms e_d, e_q on d, q axis., e_d=0, $e_q=\omega_{re}\Phi_f$. This equivalent circuit is shown in Fig.2.5. Here, v_d, v_q are d, q axis voltages, while i_d, i_q are d, q axis currents. K_E is the same as Φ_f in eq.(2.22). R_a, L_a is the same definition as eq.(2.21).

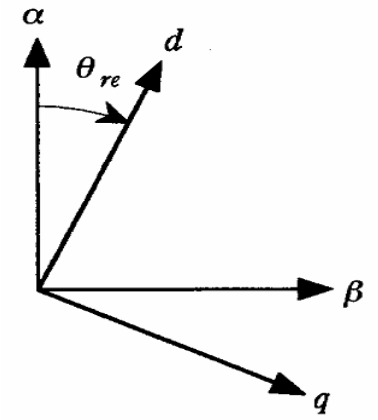

Fig.2.5 Transformation from stationary two coordinate $\alpha-\beta$ to rotated two coordinate *d*-*q*

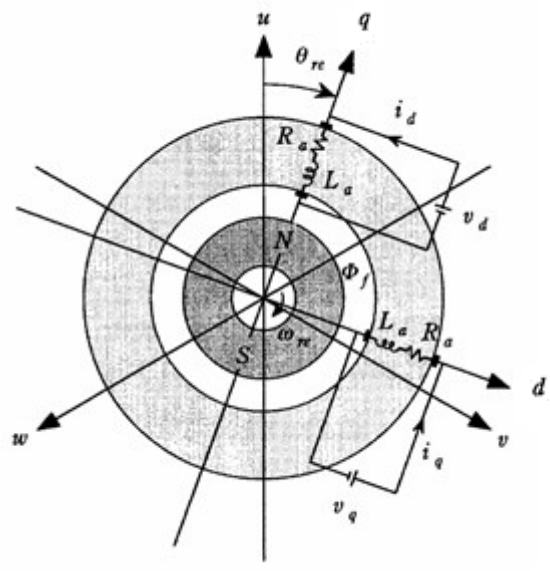

Fig.2.6 Equivalent circuit in $d-q$ axis

By implementing position sensor such as encoder, it becomes possible to detect d, q axis. If three-phase voltages or currents are sinusoidal waves, voltages or currents on d, q axis are direct signals.

With equivalent circuits of SPMSM, An equivalent circuit in 1 phase which is common used is shown in Fig.2.7. This circuit uses 3 phase voltages which has been discussed in Fig.2.3 and eq.(2.14). And it represents as the form of eq.(2.27).

$$v_u = (R_a + pL_a)i_u + e_u \tag{2.27}$$

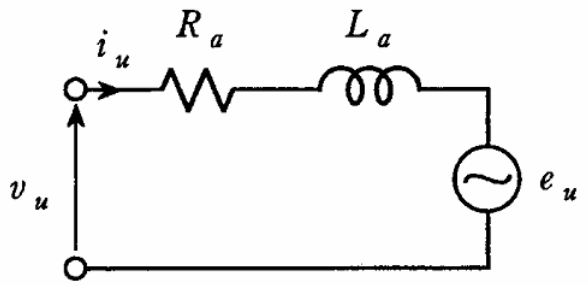

Fig.2.7 Equivalent circuit in 1 phase

In eq.(2.26), d, q axis inductances have the same value($L_d = L_q = L_a$). It represents SPMSM. When

d, *q* axis inductances are different(L_d<L_q), it represents IPMSM. In general, IPMSM voltage equation are given as eq.(2.28).

$$\begin{bmatrix} v_d \\ v_q \end{bmatrix} = \begin{bmatrix} R_\alpha + pL_d & -\omega_{re}L_q \\ \omega_{re}L_d & R_\alpha + pL_q \end{bmatrix} \begin{bmatrix} i_d \\ i_q \end{bmatrix} + \begin{bmatrix} 0 \\ \omega_{re}\phi_f \end{bmatrix} \tag{2.28}$$

In this paper, the electronics mathematics models are based on eq.(2.28).

Where,

$$\begin{bmatrix} L_d \\ L_q \\ L_0 \end{bmatrix} = \sqrt{\frac{2}{3}} \begin{bmatrix} \cos\theta_{re} & \cos\left(\theta_{re} - \frac{2}{3}\pi\right) & \cos\left(\theta_{re} + \frac{2}{3}\pi\right) \\ -\sin\theta_{re} & -\sin\left(\theta_{re} - \frac{2}{3}\pi\right) & -\sin\left(\theta_{re} + \frac{2}{3}\pi\right) \\ \frac{1}{2} & \frac{1}{2} & \frac{1}{2} \end{bmatrix} \begin{bmatrix} L_u \\ L_v \\ L_w \end{bmatrix} \tag{2.29}$$

$$\begin{bmatrix} L_u \\ L_v \\ L_w \end{bmatrix} = \begin{bmatrix} \cos\theta_{re} & -\sin\theta_{re} & 1 \\ -\cos\left(\theta_{re} - \frac{2}{3}\pi\right) & -\sin\left(\theta_{re} - \frac{2}{3}\pi\right) & 1 \\ \cos\left(\theta_{re} + \frac{2}{3}\pi\right) & -\sin\left(\theta_{re} + \frac{2}{3}\pi\right) & 1 \end{bmatrix} \begin{bmatrix} L_d \\ L_q \\ L_0 \end{bmatrix} \tag{2.30}$$

2.2.3 Dynamics of PMSM

PMSM driving torque T_e is generated by Lorentz force. IPMSM has saliency compared with SPMSM. The reluctance torque happens, meanwhile there is no saliency in SPMSM. Due to this, IPMSM driving torque T_e generated by q axis current is:

$$\begin{aligned} T_e &= P\left(\varphi_d i_q - \varphi_q i_d\right) \\ &= P\left\{\left(\phi_f + L_d i_d\right) i_q - L_q i_q i_d\right\} \\ &= P\left\{\phi_f + \left(L_d - L_q\right) i_d\right\} i_q \end{aligned} \tag{2.30}$$

To reduce the influence of reluctance torque, take $i_d = 0$. With vector control (Field Oriented Control : FOC)

$$T_e = P\phi_f i_q \tag{2.31}$$

Here, P is a number of pole-pairs. In this paper, with the condition of IPMSM vector control, Driving torque is represented as eq.(2.31).

2.3 Vector control of PMSM

In last section, the voltage equations on *d*, *q* axis has been described. In this section, the basic speed control of PMSM called vector control or FOC(Field Oriented Control) is explained.

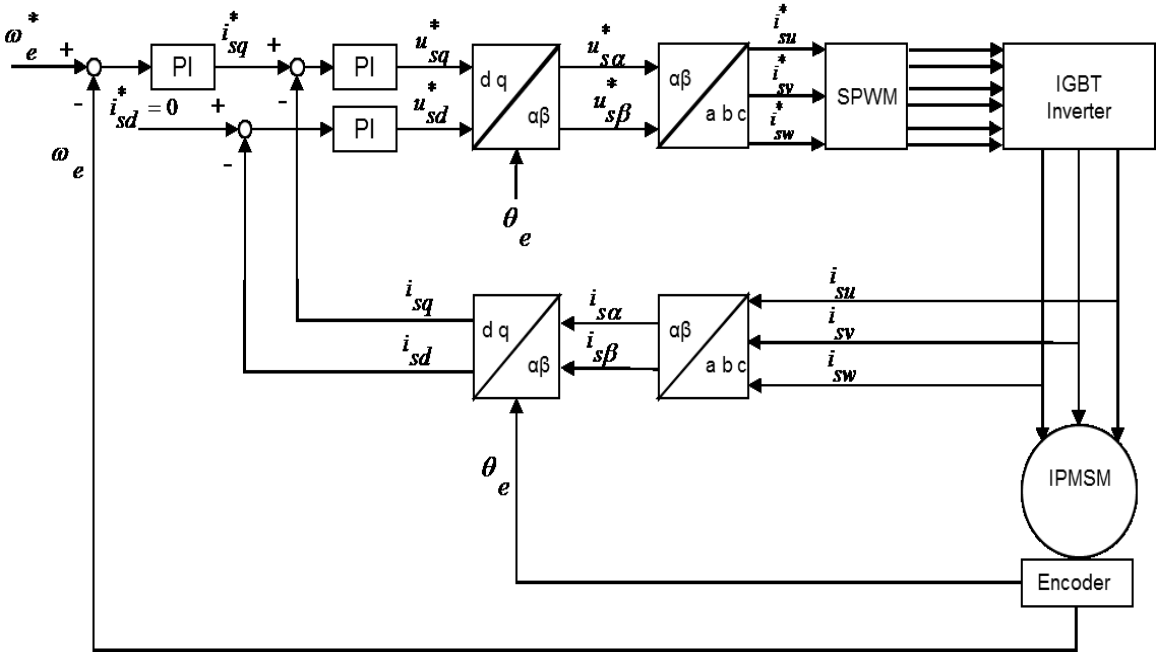

Fig.2.8 Equivalent circuit in 1 phase

Fig.(2.8) is the control block of IPMSM vector controls. In IPMSM vector controls, a position sensor such as encoder is the key to ensure the whole system responsibility, as it can detect the position and speed information.

But it should be pointed out that the method to remove encoder is the target of this research. This control is called position sensorless speed control. This part will be discussed in section2.4.

2.4 Position sensorless control method for PMSM

As referred in section2.3, this research target is position sensorless speed control for PMSM. The reasons to carry on this control has been discussed in section1.1.3. And in this control, a strategy called observer is usually applied in the whole system. The core idea of observer in position sensorless speed control for PMSM is using voltage and current signals which can be measured or calculated to rebuild PMSM speed and position signals. With these signals, whole system carries out feedback control. In other words, the target that getting rid of encoder can be achieved. The whole position sensorless speed control system for PMSM is shown in Fig.2.9.

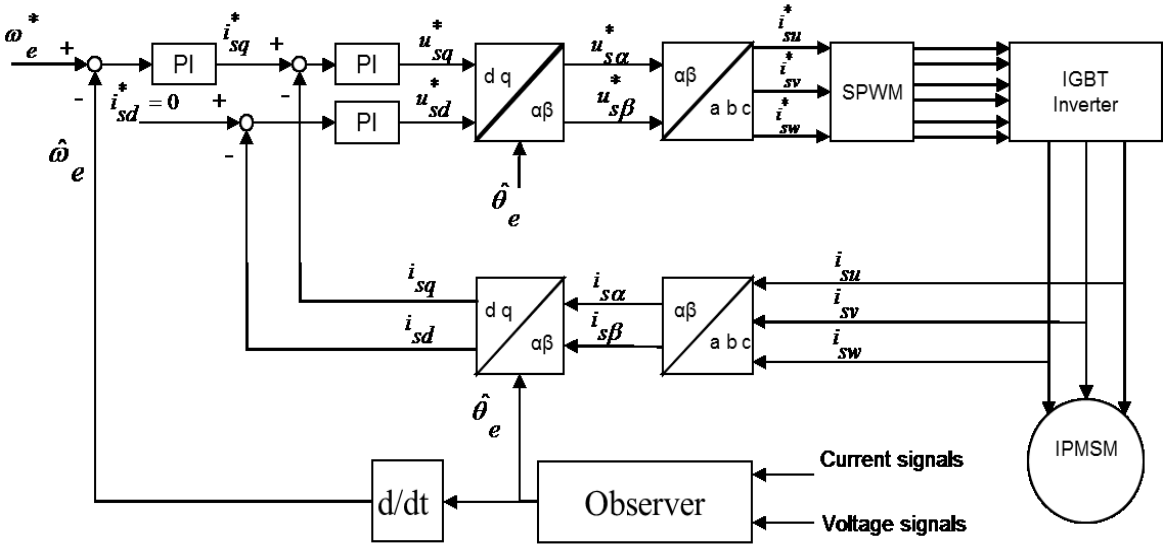

Fig.2.9 Position sensorless speed control system for PMSM

Chapter3. EEMF Observer for PMSM position sensorless control (Former method) [18][19][20]

3.1 Foreword

To achieve PMSM position sensorless speed control, just as the content has been discussed before, position information of permanent magnet on rotor is necessary. For this reason, a position sensor called encoder is applied. However, installing encoder makes the system more expensive. And in some environment, for example, high dust environment, it is impossible to install this kind of position sensor. To solve this problem, PMSM position sensorless speed control methods becomes our research target.

In this chapter, former method EEMF(Extended Electromotive Force) Observer is discussed. And the weakness of this observer will be concluded with experiment results.

3.2 Definition of EEMF Observer

To explained EEMF Observer clearly, PMSM voltage equation, which is shown in eq.(2.28),it will be listed in eq.(3.1) again to illustrate the part of basic equation of EEMF observer in Chapter 3.

$$\begin{bmatrix} v_d \\ v_q \end{bmatrix} = \begin{bmatrix} R_\alpha + pL_d & -\omega_{re}L_q \\ \omega_{re}L_d & R_\alpha + pL_q \end{bmatrix} \begin{bmatrix} i_d \\ i_q \end{bmatrix} + \begin{bmatrix} 0 \\ \omega_{re}K_E \end{bmatrix} \tag{3.1}$$

With transformation matrix[c], PMSM voltage equation on stationary two coordinate axis $(\alpha-\beta)$ is eq.(3.2).

$$\begin{bmatrix} v_\alpha \\ v_\beta \end{bmatrix} = R\begin{bmatrix} i_\alpha \\ i_\beta \end{bmatrix} + pL_0\begin{bmatrix} i_\alpha \\ i_\beta \end{bmatrix} + pL_1\begin{bmatrix} \cos 2\theta_{re} & \sin 2\theta_{re} \\ \sin 2\theta_{re} & -\cos 2\theta_{re} \end{bmatrix}\begin{bmatrix} i_\alpha \\ i_\beta \end{bmatrix} + \omega_{re}K_E\begin{bmatrix} -\sin\theta_{re} \\ \cos\theta_{re} \end{bmatrix} \tag{3.2}$$

In eq.(3.2), $L_0=(L_d+L_q)/2$, $L_1=(L_d-L_q)/2$. To IPMSM which has saliency characteristics, $L_1\neq 0$. The third section of the right part in eq.(3.2), $(2\theta_{re})$ is left. But it is better only to consider θ_{re} in EEMF Observer in eq.(3.2). For this reason, it should have some alternatives with eq.(3.2). In reference paper[10], An alternative to eliminate the term of $2\theta_{re}$ has been proposed as eq.(3.3).

$$\begin{aligned} \begin{bmatrix} v_\alpha \\ v_\beta \end{bmatrix} = R\begin{bmatrix} i_\alpha \\ i_\beta \end{bmatrix} + \begin{bmatrix} pL_d & \omega_{re}(L_d - L_q) \\ -\omega_{re}(L_d - L_q) & pL_d \end{bmatrix}\begin{bmatrix} i_\alpha \\ i_\beta \end{bmatrix} \\ + \left\{(L_d - L_q)(\omega_{re}i_d - i_q) + \omega_{re}K_E\right\}\begin{bmatrix} -\sin\theta_{re} \\ \cos\theta_{re} \end{bmatrix} \end{aligned} \tag{3.3}$$

The EEMF signal is defined as eq.(3.4). And EEMF signal is the third term of the right part in eq.(3.3).

$$\begin{bmatrix} \mathrm{e}_\alpha \\ \mathrm{e}_\beta \end{bmatrix} = \left\{(L_d - L_q)(\omega_{rfe}i_d - \dot{i}_q) + \omega_{re}K_E\right\}\begin{bmatrix} -\sin\theta_{rfe} \\ \cos\theta_{rfe} \end{bmatrix} \tag{3.4}$$

In eq.(3.4), once EEMF signal vector can be estimated, it is possible to estimate PMSM rotor position.

3.3 Control block of EEMF Observer

With eq.(3.3), PMSM linear state equation can be calculated as eq.(3.5).

$$\frac{d}{dt}\begin{bmatrix} i \\ e \end{bmatrix} = \begin{bmatrix} A_{11} & A_{12} \\ 0 & A_{22} \end{bmatrix}\begin{bmatrix} i \\ e \end{bmatrix} + \begin{bmatrix} B_1 \\ 0 \end{bmatrix} v \tag{3.5}$$

ただし

$$A_{11} = -(R / L_d)I + \{\omega_{rfe}(L_d - L_q) / L_d\}J$$
$$A_{12} = (-1 / L_d)I$$
$$A_{22} = \omega_{rfe} J$$
$$B_1 = (1 / L_d)I$$
$$I = \begin{pmatrix} 1 & 0 \\ 0 & 1 \end{pmatrix} \qquad J = \begin{pmatrix} 0 & -1 \\ 1 & 0 \end{pmatrix}$$

Output equation can be written as the type of eq.(3.6).

$$i = \begin{bmatrix} I & 0 \end{bmatrix}\begin{bmatrix} i \\ e \end{bmatrix} \tag{3.6}$$

With eq.(3.5), the minimum dimension observer to estimate PMSM EEMF voltage signal e has been established.

$$\begin{aligned} \dot{\hat{i}} &= A_{11} i + A_{12}\hat{e} + B_1 v \\ \dot{\hat{e}} &= A_{22}\dot{\hat{e}} + G(\dot{\hat{i}} - \dot{i}) \\ &= A_{11} G i + (A_{12} G + A_{22})\hat{e} + B_1 G v - G\dot{i} \end{aligned} \tag{3.7}$$

In eq.(3.7), " ^ " is the present of estimated signal, G is the observer gain which can be written as $G = g_1 I + g_2 J$. In eq.(3.7), as the differential current signal $\dot{i}$ is included, it may amplify the high frequency signal. In real system, it needs middle function, which taken as ξ を to avoid current differential signal.

$$\begin{aligned} \xi &= \hat{e} + G\dot{i} \\ \dot{\xi} &= \dot{\hat{e}} + G\dot{i} \end{aligned} \tag{3.8}$$

Take eq.(3.8) into eq.(3.7). The eq.(3.9) can be got.

$$\begin{aligned}\dot{\xi} &= (A_{12}G + A_{22})\xi + B_1 G v + G(A_{11}I - A_{12}G - A_{22})i \\ \hat{e} &= \xi - Gi\end{aligned} \tag{3.9}$$

Eq.(3.9) is the same as disturbance observer of eq.(3.7). The estimated error of EEMF voltage can be considered as $\varepsilon = \hat{e} - e$. With eq.(3.5) and (3.6)

$$\begin{aligned}\dot{\varepsilon} &= \dot{\hat{e}} - \dot{e} = (A_{22} + A_{12}G)\varepsilon \\ &= \left\{ -\frac{g_1}{L_d} I + \left(\omega_{re} - \frac{g_2}{L_d} \right) J \right\} \varepsilon\end{aligned} \tag{3.10}$$

The poles of observer are shown in Fig. 3.1. The rules of pole placement follows $-\alpha I + \beta J$. In this way,

$$\dot{\varepsilon} = \dot{\hat{e}} - \dot{e} = (-\alpha I + \beta J)\varepsilon \tag{3.11}$$

The gain of observer can be written as eq.(3.12).

$$\begin{aligned}g_1 &= \alpha L_d \\ g_2 &= (\omega_{re} - \beta) L_d\end{aligned} \tag{3.12}$$

To stabilize the observer, $\alpha > 0$. Poles are necessary to be placed in the left part of pole placement. Observer gain can be taken as eq.(3.13), with eq.(3.12). The transfer function $H_{\alpha\beta}$(s) is:

$$H_{\alpha\beta}(s) = \frac{\hat{e}}{e} = \frac{\alpha I - \beta J + \omega_{rfe} J}{(s+\alpha)^2 + \beta^2} \{ (s+\alpha) I + \beta J \} \tag{3.13}.$$

In eq.(3.13), $\beta = \omega_{re}$. Then eq.(3.14) can be got.

$$H_{\alpha\beta}(s) = \frac{\hat{e}}{e} = \frac{\alpha I}{(s+\alpha) I - \omega_{rfe} J} \tag{3.14}$$

The equivalent block of disturbance observer is in Fig.3.2. Eq.(3.14) can be taken as filter. The frequency characteristics of rotating vector ω is the bandpass filter by center frequency $\hat{\omega}_{rfe}$ with the width of α. For this reason, the low-pass filter with cut-off frequency α is shown in (3.15).

$$H_{dq}(s) = \frac{\hat{e}_{dq}}{e_{dq}} = \frac{\alpha}{s+\alpha} \tag{3.15}$$

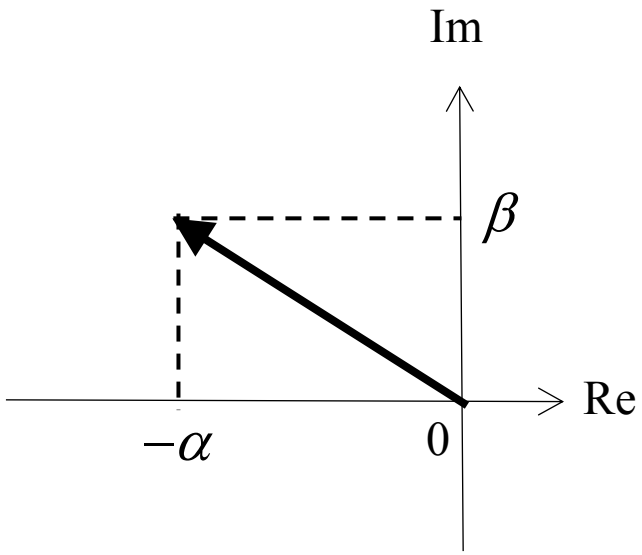

Fig.3.1 Observer pole placement

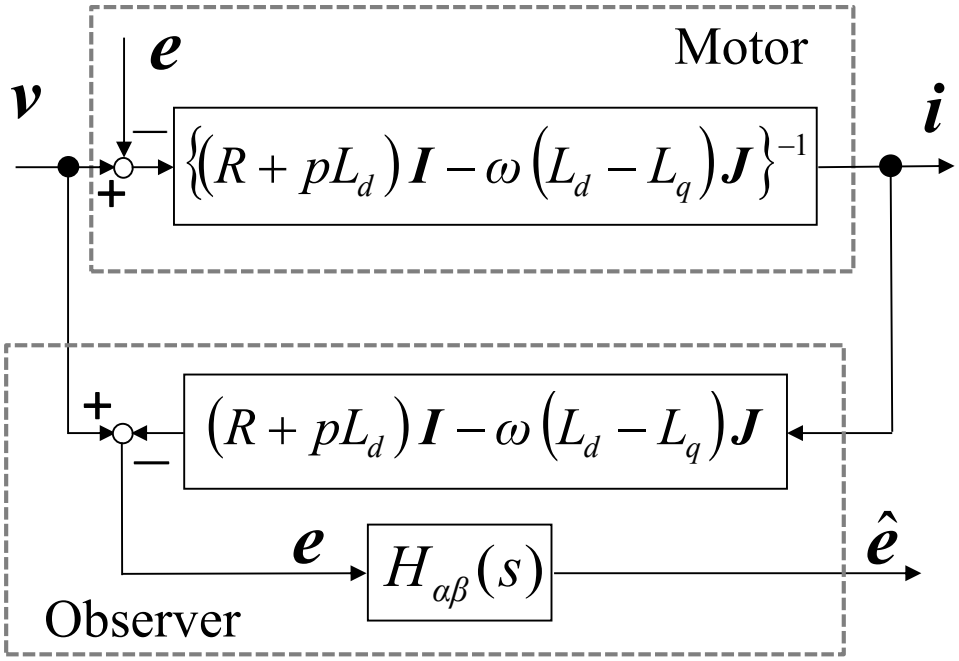

Fig.3.2 The structure of EEMF disturbance observer

The EEMF disturbance observer is given. With this observer, it becomes possible to estimate position information in eq.(3.4).

$$\theta_r = \frac{1}{P}\arctan\left(-\frac{e_\alpha}{e_\beta}\right) \tag{3.16}$$

$$\hat{\theta}_{re} = \arctan\left(-\frac{\hat{e}_\alpha}{\hat{e}_\beta}\right) \tag{3.17}$$

$$\hat{\theta}_r = \frac{\hat{\theta}_{re}}{P} \tag{3.18}$$

Speed estimated value $\hat{\omega}_{re}$ is calculated by eq.(3.15), which can be shown as eq.(3.19).

$$\hat{\omega}_{re} = \frac{s}{\varpi + 1}\hat{\theta}_{re} \tag{3.19}$$

3.4 Experiment of PMSM position sensorless control with EEMF Observer

3.4.1 Experiment parameters

To confirm the characteristics of EEMF disturbance observer of PMSM, Experiment of PMSM position sensorless speed control with EEMF Observer is carried out. The parameters of IPMSM and its control system is shown in table I.

Table I. PMSM position sensoreless speed control with EEMF Observer Parameters

Number of pole pairs	P	3
Stator Resistance	R [Ω]	1.132
d-axis inductance	L_d [H]	0.01238
q-axis inductance	L_q [H]	0.01572
EMF constant	K_E [V·s/rad]	0.211
Motor inertia	J_r [kg·m^2]	0.0055
Speed controller Proportional gain	[A · s/rad]	0.08
Speed controller Integral gain	[A/rad]	0.14
Current controller Proportional gain	[V/A]	0.01238*5000
Current controller Integral gain	[V/(A·s)]	2500
Sampling time of whole system	[ms]	0.1
Load torque	[N·m]	0.5
Pole of disturbance observer	α[rad/s]	0.5ωre
Pole of disturbance observer	B[rad/s]	ωre

3.4.2 Experiment results

(1). Situation of 600[rpm]

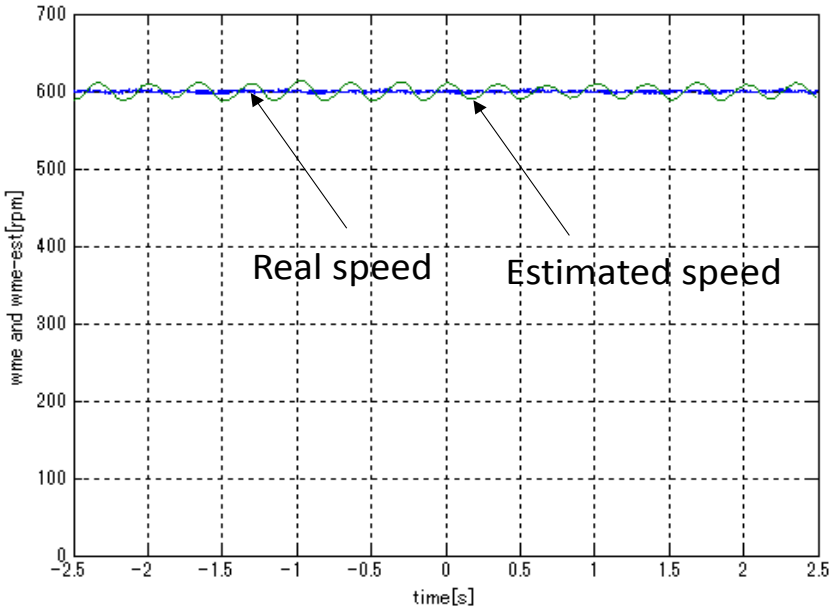

Fig.3.3 Estimated speed and real speed in 600rpm [rpm]

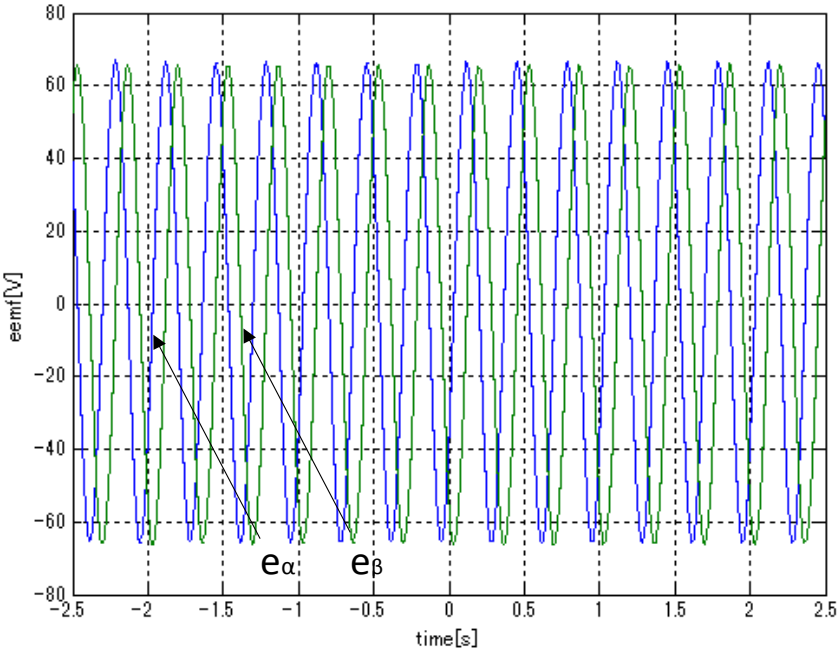

Fig.3.4 EEMF voltage signals in 600rpm [V]

(2). Situation of 500[rpm]

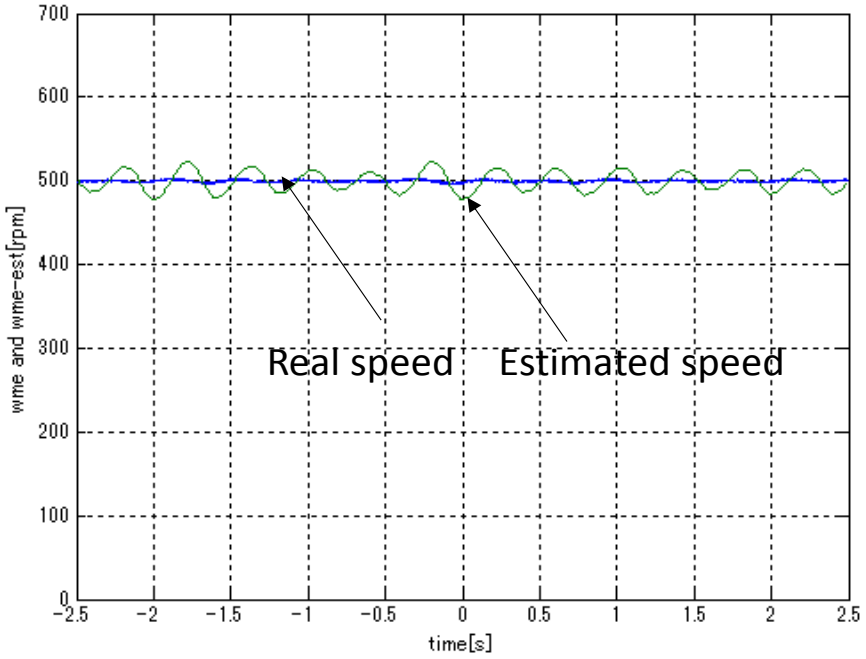

Fig.3.5 Estimated speed and real speed in 500rpm [rpm]

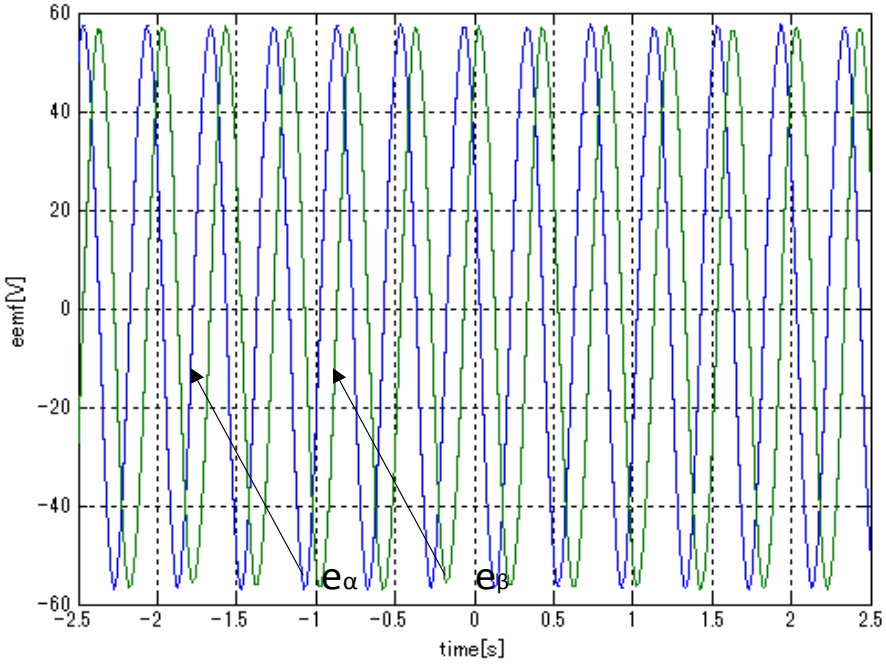

Fig.3.6 EEMF voltage signals in 500rpm [V]

(3). Situation of 350[rpm]

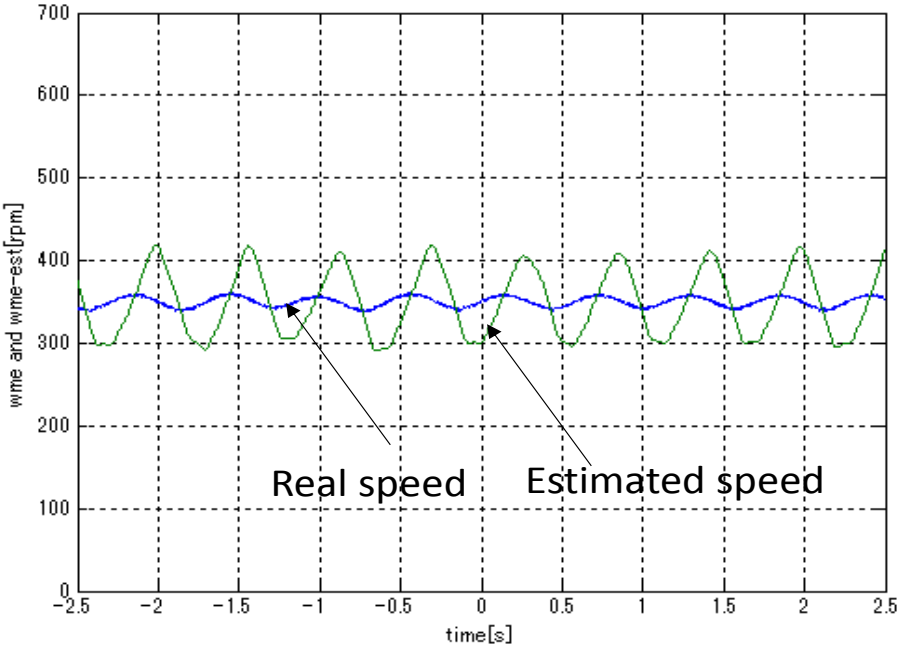

Fig.3.7 Estimated speed and real speed in 350rpm [rpm]

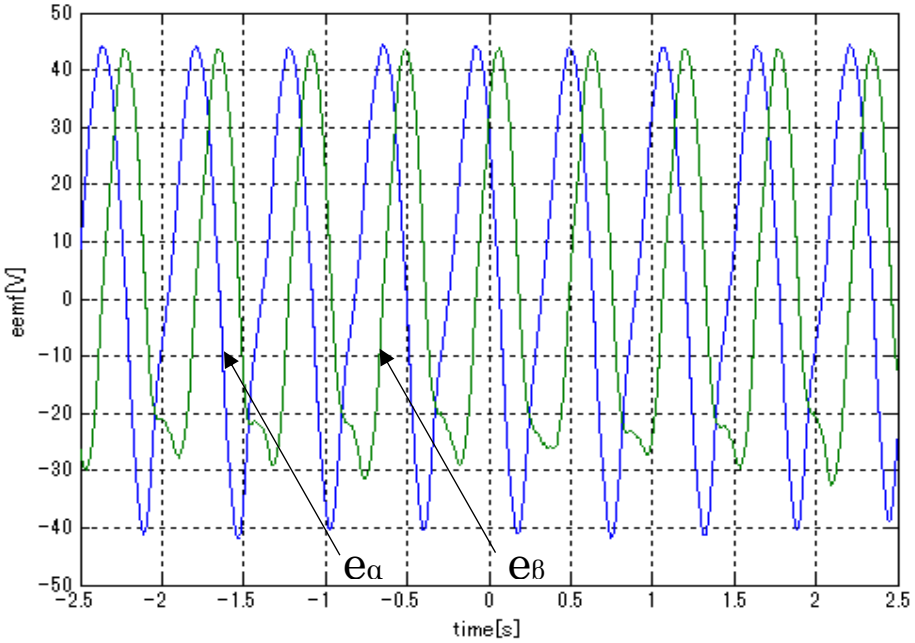

Fig.3.8 EEMF voltage signals in 350rpm [V]

(4). Speed and torque range can be controlled with EEMF Observer

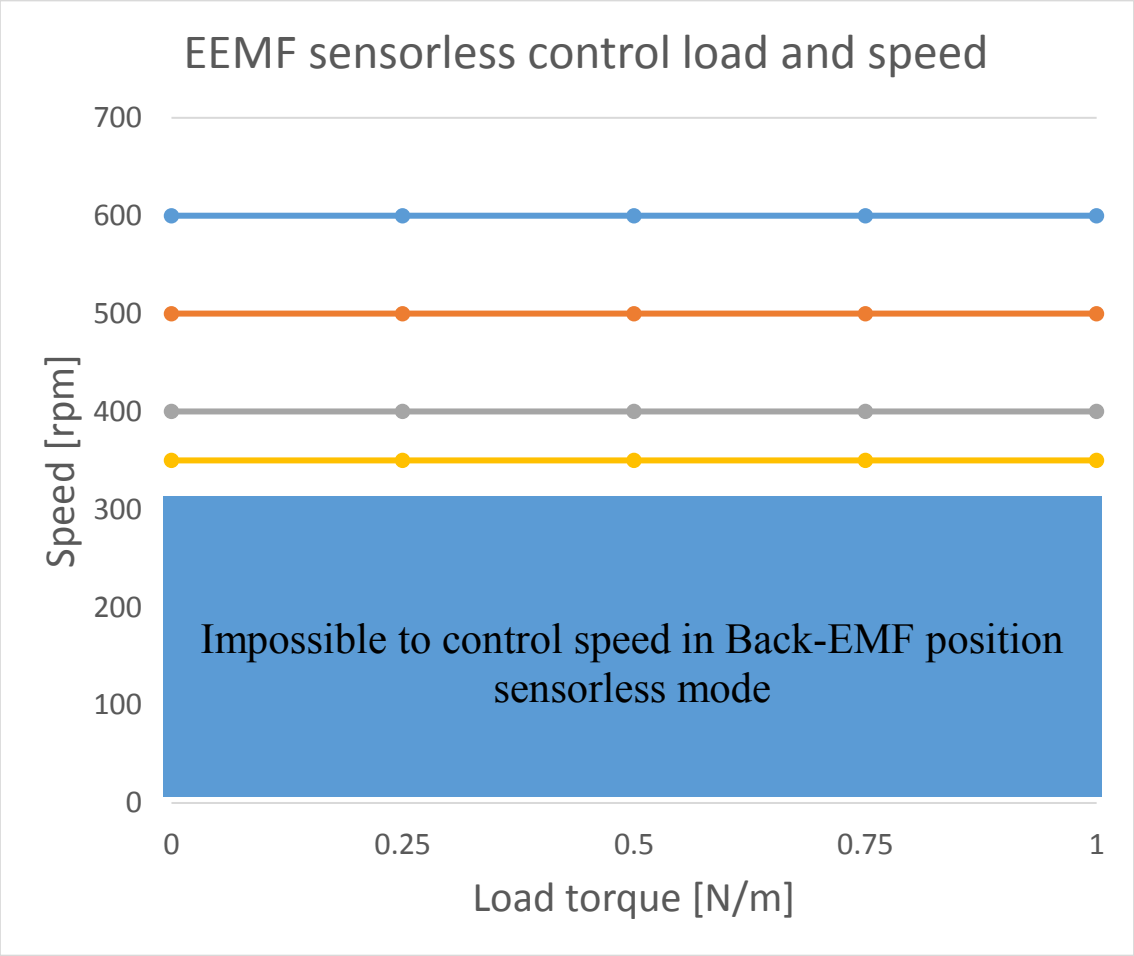

Fig.3.9 Range can be controlled with EEMF Observer

3.5 Weakness of PMSM position sensorless control with EEMF Observer

From the description in this chapter, it can be known that there are quite a lot problems in PMSM position sensorless control with EEMF Observer. The weakness of this observer is as follows:

(1). There is low-pass filter in EEMF disturbance observer. It causes phase delay.

(2). EEMF voltage signals cross zero-point, which makes the process of eq.(3.17) quite complicated in digital system.

(3). Once PMSM works in very low-speed range(ex. 60[rpm]), it is difficult to estimate EEMF voltages correctly. And this has been proved in experiment part. PMSM has the risk to be out of control when this situation happens.

To solve the problems above, a novel PMSM position sensorless speed control method called d-axis current random signal injection with EKF is researched in this paper. It will be discussed in detail from next chapter.

Chapter4. PMSM position sensorless speed control with Extended Kalman Filter (EKF)

4.1 Extended Kalman Filter(EKF)

4.1.1 Introduction of EKF

EKF(Extended Kalman Filter) is a nonlinear form of Kalman Filter[21][22], which uses linear state equation to carry out optimal estimation of system state. In Kalman Filter, input signals are applied to measure the data from varieties of sensors. Due to the white noise and disturbance in system are included in the data that measured, this optimal estimation can be considered as data filter.

Data filtering is a data processing skill to eliminate the noise and restore actual data from measurement signals. Kalman Filter can estimate the system dynamic state when measurement noise is existed in system. As it is quite easier for digital processing, and can achieve online data innovation, Kalman Filter is a popular filtering method in the field of telecommunication, navigation and system control.

In PMSM position sensorless speed control system, as motor speed, voltages and currents affect each other, it is a typical nonlinear system. As a result, EKF is applied to estimate speed and position instead of the position sensor like encoder.

4.1.2 EKF algorithm[23][24][25][26]

Kalman Filter is able to achieve optimal estimation for the target which is controlled in Gauss white noise environment. In nonlinear system, the normal method is to use linearization skill, such as taylor expansion. By this kind of linearization, nonlinear system can be almost taken as linear system. After that, Kalman Filter algorithm can be achieved to finish estimation and filtering.

(1). State equation

EKF is based on the modern control theory. As a result, Eq.(4.1) is the system state equation and measurement equation.

$$\begin{aligned} px &= f(x) + Bu \\ y &= Hx \end{aligned} \tag{4.1}$$

In eq.(4.1), where,

p ------Differential coefficient;
x ------System state;
$f(x)$ ------System nonlinear part;
B ------Input matrix;
u ------Input signals;
y ------Output signals;
H ------Output matrix.

(2). Model linearization

In the part of EKF introduction, it has been discussed that system model linearization for nonlinear control system is a necessary and very important step for EKF. Here, a linearization method called Taylor expansion is shown in eq.(4.2):

$$f(x)=\frac{f(x_0)}{0!}+\frac{f'(x_0)}{1!}(x-x_0)+\ldots+\frac{f^{(n)}(x_0)^n}{n!}(x-x_0)^n+R_n(x) \tag{4.2}$$

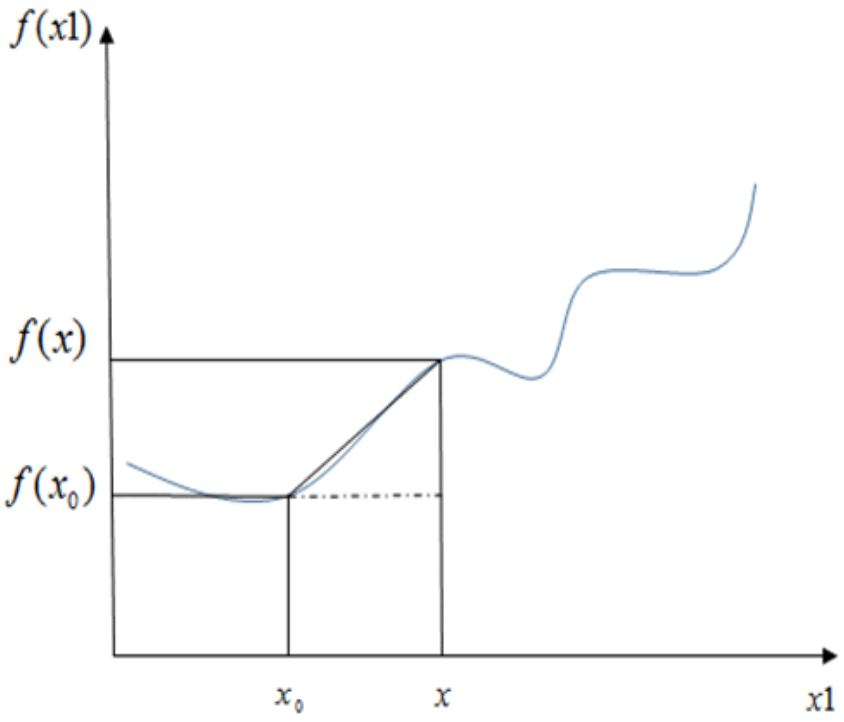

Fig.4.1 System linearization

In Fig.4.1, it is easy to see if $(x-x_0)$ is small enough, it can be considered that first order differential coefficient is efficient to linearize the system model. Eq.(4.2) can be approximately written as:

$$f(x)=\frac{f(x_0)}{0!}+\frac{f'(x_0)}{1!}(x-x_0) \tag{4.3}$$

(3). Model discretization

Eq.(4.1) is the state equation based on continuous system, which means the sampling time is 0. It is impossible for digital system such as MCU(Micro Controller Unit) to control the system in such a short time. As a result, system model discretization for continuous system is necessary. And it is shown in eq.(4.4).

$$\begin{aligned} x_k &= A_k x_{k-1} + B_k u_{k-1} \\ y_k &= H_k x_{k-1} \end{aligned} \tag{4.4}$$

In eq.(4.4), where,

x_k ------System state at time k;

x_{k-1} ------System state at time k-1;

A_k ------System state matrix at time k;

B_{k-1} ------Input matrix at time k-1;

u_{k-1} ------Input signals at time k-1 ;

y_k ------Output signals at time k;

H_k ------Output matrix at time k.

After model discretization is finished, EKF algorithm can be carried out. It consists of two parts, time innovation and measurement innovation. Time innovation is calculated for estimated state of the system, while measurement innovation data is updated by comparing data from sensor with time innovation data. They are shown in eq.(4.5) and eq(4.6).

(4) Time innovation

$$\begin{aligned} \hat{x}_{k/k-1} &= A_k x_{k-1} + Bu_{k-1} \\ P_{k/k-1} &= A_k P_{k-1} A_k^T + Q \end{aligned} \tag{4.5}$$

(5) Measurement innovation

$$\begin{aligned} K_k &= \frac{P_{k/k-1} H_k^T}{H_k P_{k/k-1} H_k^T + R} \\ P_k &= (I - K_k H_k) P_{k/k-1} \\ \hat{x}_k &= \hat{x}_{k/k-1} + K_k [y_k - H_k \hat{x}_{k/k-1}] \end{aligned} \tag{4.6}$$

In eq.(4.5) and eq.(4.6),

$\hat{x}_k$ ------System state which has been innovated at time k;

$\hat{x}_{k/k-1}$ ------System state which is innovated from time k-1 to time k;

P_k ------System error which has been innovated at time k;

$P_{k/k-1}$ ------System error which has been innovated from time k-1 to time k;

P_{k-1} ------ System error which at time k-1 ;

K_k ------Kalman gain at time k ;

Q ------System state noise balanced matrix;

R ------System measurement sensor noise balanced matrix.

4.2 EKF Observer for PMSM position sensorless speed control

From eq.(3.1), it is easy to be seen that PMSM voltage equation is a typical nonlinear system, for the reason that the voltage values on d-axis and q-axis are influenced not only by currents, but also the PMSM electrical speed. At the same time, d-axis current impacts on q-axis voltage, while q-axis current impacts on d-axis voltage, respectively.

In order to apply Kalman Filter to achieve PMSM position sensorless speed control, nonlinear form of Kalman Filter, EKF is chosen to establish PMSM speed and position observer to carry out position sensorless speed control.

In EKF observer, PMSM voltage equation will be applied to achieve EKF algorithm, as the contents in section 4.1. In this section, firstly, EKF observer mathematics models for PMSM will be carried out. After that, the whole EKF position sensorless speed control block figure will be given.

4.2.1 EKF observer mathematics models for PMSM

IPMSM mathematics model is written as:

$$\begin{bmatrix} v_d \\ v_q \end{bmatrix} = \begin{bmatrix} R_\alpha + pL_d & -\omega_{re}L_q \\ \omega_{re}L_d & R_\alpha + pL_q \end{bmatrix} \begin{bmatrix} i_d \\ i_q \end{bmatrix} + \begin{bmatrix} 0 \\ \omega_{re}K_E \end{bmatrix} \tag{4.7}$$

From eq.(4.7), it can be rewritten as eq.(4.8).

$$\begin{bmatrix} pi_d \\ pi_q \end{bmatrix} = \begin{bmatrix} -\frac{R_\alpha}{L_d} & \frac{L_q}{L_d}\omega_{re} \\ -\frac{L_d}{L_q}\omega_{re} & -\frac{R_\alpha}{L_q} \end{bmatrix} \begin{bmatrix} i_d \\ i_q \end{bmatrix} + \begin{bmatrix} \frac{u_d}{L_d} \\ -\frac{\omega_{re}K_E}{L_q} + \frac{u_q}{L_q} \end{bmatrix} \tag{4.8}$$

The differential form of IPMSM for EKF is as follows:

$$\begin{cases} pi_d = -\frac{R_\alpha}{L_d}i_d + \frac{L_q}{L_d}\omega_{re}i_q + \frac{u_d}{L_d} \\ pi_q = -\frac{L_d}{L_q}\omega_e i_d - \frac{R_\alpha}{L_q}i_q - \frac{\omega_{re}K_E}{L_q} + \frac{u_q}{L_q} \\ p\omega_{re} = 0 \\ p\theta_{re} = \omega_{re} \end{cases} \tag{4.9}$$

As EKF algorithm in section 4.1.2, EKF for IPMSM algorithm consists of the following 5 parts:

(1). State equation of IPMSM

$$\begin{bmatrix} pi_d \\ pi_q \\ p\omega_{re} \\ p\theta_{re} \end{bmatrix} = \begin{bmatrix} -\frac{R_\alpha}{L_d}i_d + \frac{L_q}{L_d}\omega_{re}i_q \\ -\frac{L_d}{L_q}\omega_{re}i_d - \frac{R_\alpha}{L_q}i_q - \frac{\omega_{re}K_E}{L_q} \\ 0 \\ \omega_{re} \end{bmatrix} + \begin{bmatrix} \frac{1}{L_d} & 0 \\ 0 & \frac{1}{L_q} \\ 0 & 0 \\ 0 & 0 \end{bmatrix} \begin{bmatrix} u_d \\ u_q \end{bmatrix} \tag{4.10}$$

Where the measurement equation is shown as:

$$\begin{bmatrix} i_d \\ i_q \end{bmatrix} = \begin{bmatrix} 1 & 0 & 0 & 0 \\ 0 & 1 & 0 & 0 \end{bmatrix} \begin{bmatrix} i_d \\ i_q \\ \omega_{re} \\ \theta_{re} \end{bmatrix} \tag{4.11}$$

(2). Model linearization of IPMSM

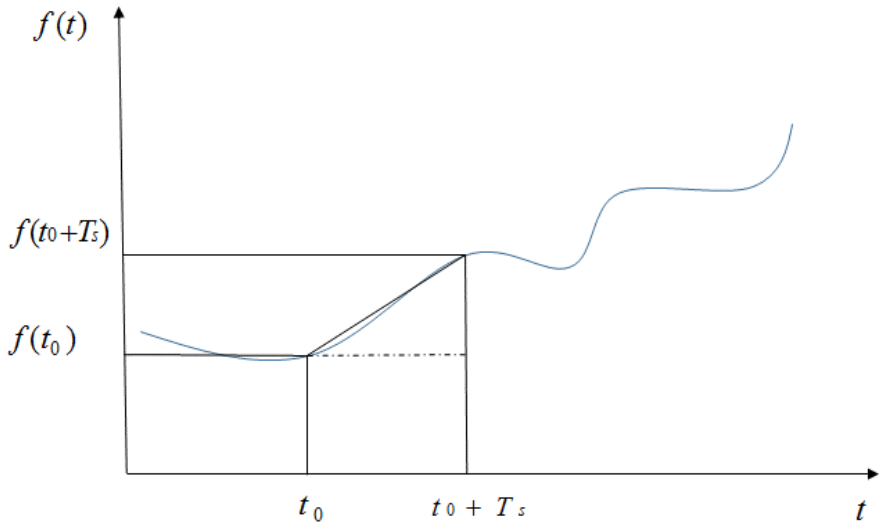

Fig.4.2 Sampling time based system linearization

From eq.(4.3), it is easy to know that:

$$f(t+T_s)=\frac{f(t)}{0!}+\frac{f'(t)}{1!}(T_s) + \ldots+\frac{f^{(n)}(t)^n}{n!}(T_s)^n+R_n(t+T_s) \tag{4.12}$$

Once the sampling time T_s is small enough, eq.(4.12) can be similarly considered as:

$$f(t+T_s)=\frac{f(t)}{0!}+\frac{f'(t)}{1!}(T_s)=f(t)+FT_s \tag{4.13}$$

Where, the first order differential coefficient is written as:

$$f'(t)=FT_s \tag{4.14}$$

(3). Model discretization of IPMSM

In the model of IPMSM, $x=[i_d \quad i_q \quad \omega_{re} \quad \theta_{re}]^T$. As a result:

$$F=\frac{\partial f(x)}{\partial x}=\begin{bmatrix} -\frac{R}{L_d} & \frac{L_q}{L_d}\omega_e & i_q\frac{L_q}{L_d} & 0 \\ -\frac{L_d}{L_q}\omega_e & -\frac{R_s}{L_q} & -\frac{L_d i_d+K_E}{L_q} & 0 \\ 0 & 0 & 0 & 0 \\ 0 & 0 & 1 & 0 \end{bmatrix} \tag{4.15}$$

The discrete state equation is as follows:

$$\begin{aligned} x_k &= A_k x_{k-1}+B_k T_s u_{k-1} \\ y_k &= H_k x_k \end{aligned} \tag{4.16}$$

In eq.(4.16),

$$A_k = I + T_s F \tag{4.17}$$

At last, discretization form of IPMSM state equation can be written as:

$$\begin{bmatrix} i_d(k) \\ i_q(k) \\ \omega_{re}(k) \\ \theta_{re}(k) \end{bmatrix}=\begin{bmatrix} 1-\frac{R_\alpha}{L_d}T_s & \frac{L_q}{L_d}\omega_{re}(k-1)T_s & i_q(k-1)\frac{L_q}{L_d}T_s & 0 \\ -\frac{L_d}{L_q}\omega_{re}(k-1)T_s & 1-\frac{R_\alpha}{L_q}T_s & -\frac{L_d i_d(k-1)+K_E}{L_q}T_s & 0 \\ 0 & 0 & 1 & 0 \\ 0 & 0 & T_s & 1 \end{bmatrix}\begin{bmatrix} i_d(k-1) \\ i_q(k-1) \\ \omega_{re}(k-1) \\ \theta_{re}(k-1) \end{bmatrix} + \begin{bmatrix} \frac{T_s}{L_d} & 0 \\ 0 & \frac{T_s}{L_q} \\ 0 & 0 \\ 0 & 0 \end{bmatrix}\begin{bmatrix} u_d(k-1) \\ u_q(k-1) \end{bmatrix} \tag{4.18}$$

While the measurement equation is written as:

$$\begin{bmatrix} i_d(k) \\ i_q(k) \end{bmatrix}=\begin{bmatrix} 1 & 0 & 0 & 0 \\ 0 & 1 & 0 & 0 \end{bmatrix}\begin{bmatrix} i_d(k) \\ i_q(k) \\ \omega_{re}(k) \\ \theta_{re}(k) \end{bmatrix} \tag{4.19}$$

(4) Time innovation

$$\begin{aligned} \hat{x}_{k/k-1} &= A_k x_{k-1} + Bu_{k-1} \\ P_{k/k-1} &= A_k P_{k-1} A_k^T + Q \end{aligned} \tag{4.20}$$

(5) Measurement innovation

$$\begin{aligned} K_k &= \frac{P_{k/k-1} H_k^T}{H_k P_{k/k-1} H_k^T + R} \\ P_k &= (I - K_k H_k) P_{k/k-1} \\ \hat{x}_k &= \hat{x}_{k/k-1} + K_k [y_k - H_k \hat{x}_{k/k-1}] \end{aligned} \tag{4.21}$$

In eq.(4.5) and eq.(4.6),

$\hat{x}_k$ ------$[\hat{i}_d(k) \;\; \hat{i}_q(k) \;\; \hat{\omega}_{re}(k) \;\; \hat{\theta}_{re}(k)]^T$;

$\hat{x}_{k/k-1}$ ------$[\hat{i}_d(k/k-1) \;\; \hat{i}_q(k/k-1) \;\; \hat{\omega}_{re}(k/k-1) \;\; \hat{\theta}_{re}(k/k-1)]^T$;

P_k ------System error which has been innovated at time k, 4*4matrix;

$P_{k/k-1}$ ------System error which has been innovated from time k-1 to time k, 4*4matrix;

P_{k-1} ------System error which at time k-1, 4*4 matrix;

K_k ------Kalman gain at time k, 4*2 matrix;

Q ------System state noise balanced matrix, 4*4 matrix;

R ------System measurement sensor noise balanced matrix, 2*2 matrix.

The contents above is the EKF Observer algorithm for IPMSM Position sensorless speed control. And the whole control system is shown in section 4.2.2.

4.2.2 Block figure of whole control system

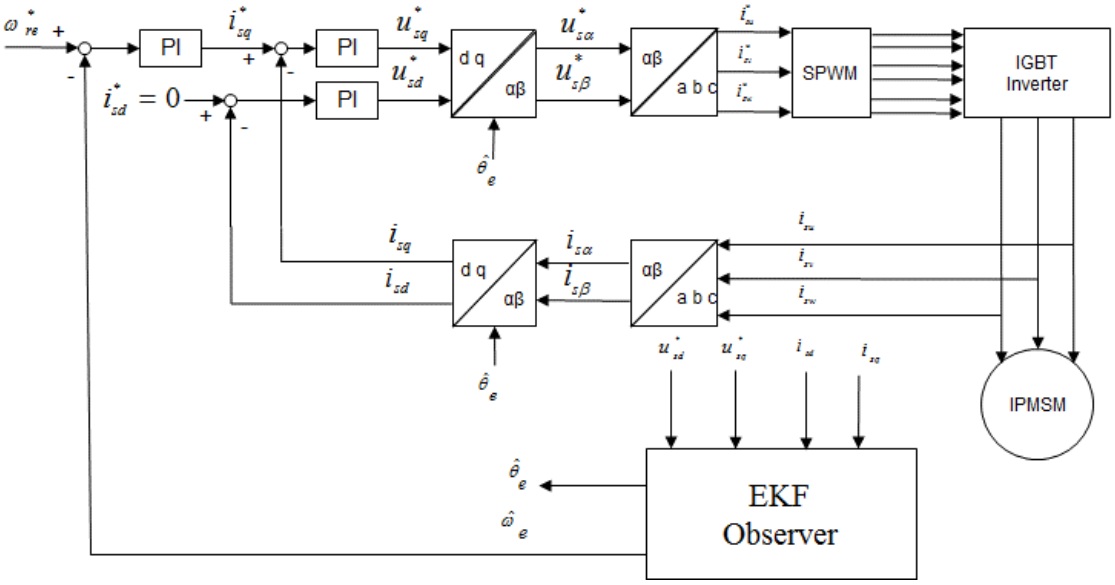

Fig.4.3 Block figure for IPMSM position sensorless speed control system

4.3 d-axis current random signal injection with EKF

4.3.1 d-axis current random signal injection EKF for PMSM position sensorless control

(1). d-axis current random signal injection

For speed or position observers in IPMSM position sensorless speed control system, such as EEMF observer, the reason why it is difficult to estimate and control the motor speed and angle is that when motor runs in low-speed range, for example, speed nearly 0[rpm], speed signal and the reference term such as EEMF voltage becomes quite small. This appearance increases the difficulty to detect such a kind of signal.

To IPMSM position sensorless speed control in low-speed range, injecting high-frequency signal is a way to estimate IPMSM speed, because the signal can be taken out after feedback, but it needs bandpass filter, which causes phase delay and usually this extracted signal is very small. It makes control system very difficult to catch this signal.

In EKF, low-speed problem still exists. But which is different from other observers, EKF can work in high noise environment, if this kind of noise is white noise. As a result, speed signal amplification becomes possible, because currents on d-axis or q-axis can be injected with white noise. Once white noise is injected in current command, speed signals will be forced to be changed, The random noise exits on IPMSM speed and position will be eliminated by EKF algorithm.

The reason of injecting signal on d-axis current is that if white random noise is added on q-axis current, it will cause the unstability when load torque suddenly added or extracted.

The amplified figure of injected signal part is shown as Fig4.4.

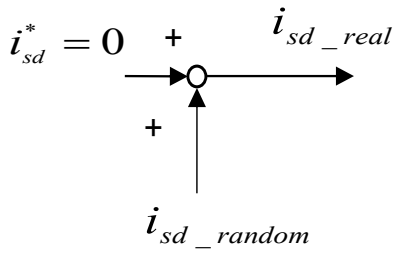

Fig.4.4 Amplified figure of injected signal part on d-axis current command

From Fig.4.4, it is easy to see:

$$i_{sd\_real}=i_{sd}^{*}+i_{sd\_random} \tag{4.22}$$

In the signal of eq.(4.22), d-axis current in PMSM includes high-frequency signal, which will be solved by EKF. Whole system state Observer judgement equation can be shown as:

$$\begin{aligned}
&\dot{x}=Ax+Bu\\
&\dot{\hat{x}}=A\hat{x}+Bu+K(y-H\hat{x})\\
&e=x-\hat{x}\\
&\dot{e}=\dot{x}-\dot{\hat{x}}
\end{aligned} \tag{4.23}$$

Where, e is the state error between real state and estimated state. When time tends to infinite, e should be 0. $\dot{e}$ is the differential form of state error, which is an alternative method to make the system stable. The detail form of eq.(4.23) for PMSM model is written as:

$$\begin{bmatrix} pi_d \\ pi_q \\ p\omega_{re} \\ p\theta_{re} \end{bmatrix}=\begin{bmatrix} -\frac{R_\alpha}{L_d}(i_d+i_{sd\_random})+\frac{L_q}{L_d}\omega_{re}i_q \\ -\frac{L_d}{L_q}\omega_{re}(i_d+i_{sd\_random})-\frac{R_\alpha}{L_q}i_q-\frac{\omega_{re}K_E}{L_q} \\ 0 \\ \omega_{re} \end{bmatrix}+\begin{bmatrix} \frac{1}{L_d} & 0 \\ 0 & \frac{1}{L_q} \\ 0 & 0 \\ 0 & 0 \end{bmatrix}\begin{bmatrix} u_d \\ u_q \end{bmatrix} \tag{4.24}$$

$$\begin{bmatrix} p\hat{i}_d \\ p\hat{i}_q \\ p\hat{\omega}_{re} \\ p\hat{\theta}_{re} \end{bmatrix} = \begin{bmatrix} -\frac{R_\alpha}{L_d}\hat{i}_d + \frac{L_q}{L_d}\hat{\omega}_{re}\hat{i}_q \\ -\frac{L_d}{L_q}\hat{\omega}_{re}\hat{i}_d - \frac{R_\alpha}{L_q}\hat{i}_q - \frac{\hat{\omega}_{re}K_E}{L_q} \\ 0 \\ \hat{\omega}_{re} \end{bmatrix} + \begin{bmatrix} \frac{1}{L_d} & 0 \\ 0 & \frac{1}{L_q} \\ 0 & 0 \\ 0 & 0 \end{bmatrix} \begin{bmatrix} u_d \\ u_q \end{bmatrix} + \begin{bmatrix} K_{K\_11} & K_{K\_12} \\ K_{K\_21} & K_{K\_22} \\ K_{K\_31} & K_{K\_32} \\ K_{K\_41} & K_{K\_42} \end{bmatrix} \begin{bmatrix} (i_d + i_{sd\_random}) - \hat{i}_d \\ i_q - \hat{i}_q \end{bmatrix} \tag{4.25}$$

Where,

random ------System injected random signal;

After calculation of the first row in eq.(4.24) and eq.(4.25), respectively, speed error can be written as:

$$e_{\omega_{re}} = \frac{R_\alpha - K_{K\_11}}{L_q i_q} i_{sd\_random} + K_{K\_12}\frac{L_d}{L_q}\left(\frac{i_q}{\hat{i}_q} - 1\right) \tag{4.26}$$

Once K_{K_11} and K_{K_12} can be set properly, when time tends to be infinite, $e_{\omega_{re}}$ will tend to be 0.

$$e_{\theta_{re}} = \int e_{\omega_{re}} dt \tag{4.27}$$

As $e_{\omega_{re}}$ tends to be 0, $e_{\theta_{re}}$ will also tend to be 0.

After calculation of the third and fourth row in eq.(4.24) and eq.(4.25), respectively, speed error and position error differential can be written as:

$$\dot{e}_{\omega_{re}} = K_{K\_31} i_{sd\_random} \tag{4.28}$$

$$\dot{e}_{\theta_{re}} = K_{K\_41} i_{sd\_random} \tag{4.29}$$

It can be seen from the first row in eq.(4.22) that $e_{\omega re}$ and $e_{\theta re}$ tends to be zero, if Kalman gain K_{K_11} and K_{K_12} can be set properly. This proper method is changing matrix Q by trail and error. The observer error turns to be zero, when time tends to be infinite.

Eq.(4.28) and eq.(4.29) means that with proper alternative by Kalman gain K_{K_31} and K_{K_41}, EKF algorithm can reduce the difference between estimated signal, such as estimated speed signal, estimated position signal and real one.

(2). Q-compensation in EKF

In former EKF for PMSM position sensorless speed control system, state noise balanced matrix Q in eq.(4.20) is usually set as diagonal matrix, because it is considered that the system states don't interfere each other. To a nonlinear system which has been linearized, this theory can be accepted. But in the novel system this research, as d-axis current is injected by white random noise, it would be better to adjust the term in matrix Q, the term which is infected by motor speed and position while impact on them. The calculation of impacts of matrix Q is as follows:

From eq.(4.20), it can be written as:

$$\begin{aligned}\hat{x}_k &= \hat{x}_{k/k-1} + K_k[y_k - H_k\hat{x}_{k/k-1}] \\ &= \begin{bmatrix}\hat{i}_{d\_k}\\ \hat{i}_{q\_k}\\ \hat{\omega}_{e\_k}\\ \hat{\theta}_{e\_k}\end{bmatrix} = \begin{bmatrix}\hat{i}_{d\_k-1}\\ \hat{i}_{q\_k-1}\\ \hat{\omega}_{e\_k-1}\\ \hat{\theta}_{e\_k-1}\end{bmatrix} + \begin{bmatrix}K_{k\_11}(i_{d\_k-1}-\hat{i}_{d\_k-1}) + K_{k\_12}(i_{q\_k-1}-\hat{i}_{q\_k-1})\\ K_{k\_21}(i_{d\_k-1}-\hat{i}_{d\_k-1}) + K_{k\_22}(i_{q\_k-1}-\hat{i}_{q\_k-1})\\ K_{k\_31}(i_{d\_k-1}-\hat{i}_{d\_k-1}) + K_{k\_31}(i_{q\_k-1}-\hat{i}_{q\_k-1})\\ K_{k\_41}(i_{d\_k-1}-\hat{i}_{d\_k-1}) + K_{k\_42}(i_{q\_k-1}-\hat{i}_{q\_k-1})\end{bmatrix}\end{aligned} \tag{4.30}$$

Combine eq.(4.20) and eq.(4.21),

$$\begin{aligned}K_k &= (P_{k/k-1}H_k^T)/(H_kP_{k/k-1}H_k^T + R) \\ &= \begin{bmatrix}K_{k\_11} & K_{k\_12}\\ K_{k\_21} & K_{k\_22}\\ K_{k\_31} & K_{k\_32}\\ K_{k\_41} & K_{k\_42}\end{bmatrix} \\ &= \begin{bmatrix}\frac{-P_{11}P_{22}}{P_{11}P_{22}-P_{12}P_{21}} + R_{11}P_{11} + \frac{P_{12}P_{21}}{P_{11}P_{22}-P_{12}P_{21}} & \frac{P_{11}P_{12}}{P_{11}P_{22}-P_{12}P_{21}} - \frac{P_{11}P_{12}}{P_{11}P_{22}-P_{12}P_{21}} + R_{22}P_{12}\\ \frac{-P_{21}P_{22}}{P_{11}P_{22}-P_{12}P_{21}} + R_{11}P_{21} + \frac{P_{12}P_{21}}{P_{11}P_{22}-P_{12}P_{21}} & \frac{P_{12}P_{21}}{P_{11}P_{22}-P_{12}P_{21}} - \frac{P_{11}P_{22}}{P_{11}P_{22}-P_{12}P_{21}} + R_{22}P_{22}\\ \frac{-P_{31}P_{22}}{P_{11}P_{22}-P_{12}P_{21}} + R_{11}P_{31} + \frac{P_{32}P_{21}}{P_{11}P_{22}-P_{12}P_{21}} & \frac{P_{12}P_{31}}{P_{11}P_{22}-P_{12}P_{21}} - \frac{P_{11}P_{32}}{P_{11}P_{22}-P_{12}P_{21}} + R_{22}P_{32}\\ \frac{-P_{22}P_{41}}{P_{11}P_{22}-P_{12}P_{21}} + R_{11}P_{41} + \frac{P_{21}P_{42}}{P_{11}P_{22}-P_{12}P_{21}} & \frac{P_{12}P_{41}}{P_{11}P_{22}-P_{12}P_{21}} - \frac{P_{11}P_{42}}{P_{11}P_{22}-P_{12}P_{21}} + R_{22}P_{42}\end{bmatrix}\end{aligned} \tag{4.31}$$

Which should be pointed out is in eq.(4.31), K_{k_12} and K_{k_21} is considered as 0, as matrix R is nearly 0.

The matrix Q is shown as eq.(4.32). Because the influence of d-axis current to speed and position should be considered, terms of Q_{13}, Q_{14} are assembled in eq.(4.32).

$$Q = \begin{bmatrix} Q_{11} & 0 & Q_{13} & Q_{14} \\ 0 & Q_{22} & 0 & 0 \\ Q_{13} & 0 & Q_{33} & 0 \\ Q_{14} & 0 & 0 & Q_{44} \end{bmatrix} \tag{4.32}$$

After proper calculation from eq.(4.20) to eq.(4.31), combine with eq.(4.32),

$$K_{k\_31} = \frac{T_s i_q (\frac{L_q}{L_d}) P_{33} + Q_{13}}{P_{11}} \tag{4.33}$$

$$K_{k\_41} = \frac{T_s^2 i_q (\frac{L_q}{L_d}) P_{33} + Q_{14}}{P_{11}} \tag{4.34}$$

It can be seen that the Kalman gain in IPMSM speed and position is impacted by terms of Q_{13}, Q_{14}. At the same time, when q-axis current changes, compensating these four terms will help IPMSM position sensorless speed control works more correctly than before. But which should be pointed out is that the rules of deciding Kalman gain K_k is still under researched. This paper will use the method of try and error to compensate the four terms of matrix Q.

The novel system block is shown in Fig.4.5.

4.3.2 Block figure of whole control system

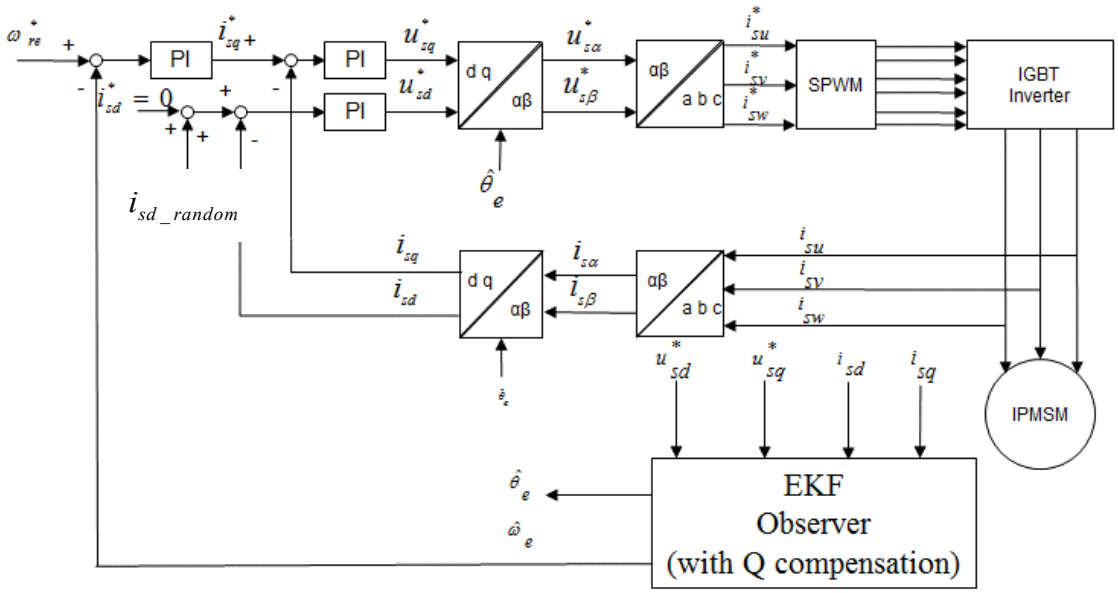

Fig.4.5 Block figure for IPMSM position sensorless speed control system with d-axis current random signal injection

The difference between system in Fig4.5 and the one in Fig.4.3 is that:

(1). In the system of Fig.4.5, the white random signal, which effective value is 0.2 is injected on d-axis current command, while the system of Fig.4.3.

(2). EKF Observer in Fig.4.5 compensates the four terms of Q matrix in algorithm, while Q matrix in Fig.4.3 is a diagonal matrix.

Chapter5. PMSM position sensorless speed control with EKF Simulation

5.1 Simulation public parameters

Table II. Simulation public parameters for EKF PMSM position sensorless speed control

Number of pole pairs	P	3
Stator Resistance	Rα [Ω]	1.132
d-axis inductance	L_d [H]	0.01238
q-axis inductance	L_q [H]	0.01572
EMF constant	K_E [V·s/rad]	0.211
Motor inertia	J_r [kg·m^2]	0.0055
Command	ω_e* [rpm]	60
Speed controller Proportional gain	[A · s/rad]	0.08
Speed controller Integral gain	[A/rad]	0.14
Current controller Proportional gain	[V/A]	0.01238*5000
Current controller Integral gain	[V/(A·s)]	2500
Supply DC voltage	[V]	20
Sampling time of whole system	[ms]	0.01
Load torque(0-1s)	[N·m]	0
Load torque(1-5s)	[N·m]	0.5 or 1
Whole simulation time	[s]	5

5.2 Simulation block figure

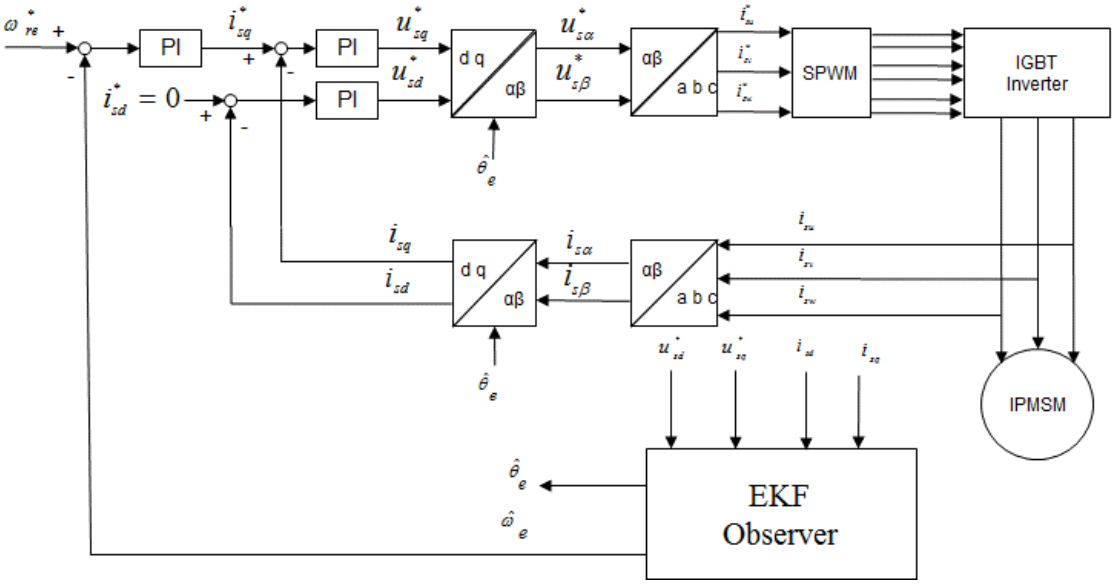

Fig.5.1 Simulation model I

(no white random signal injection, no Q compensation)

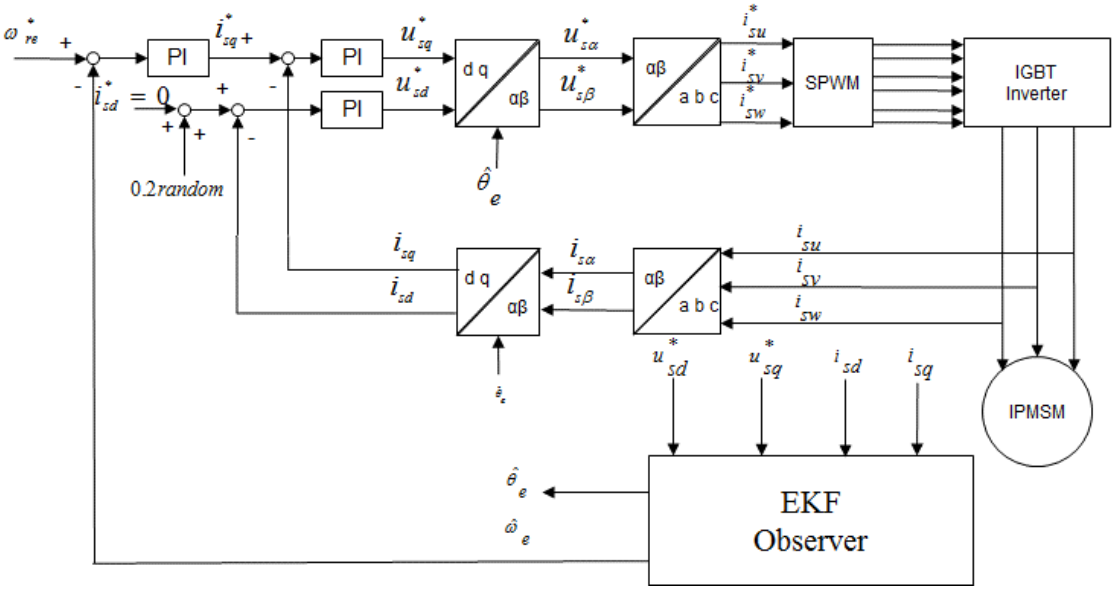

Fig.5.2 Simulation model II

(white random signal injection, no Q compensation)

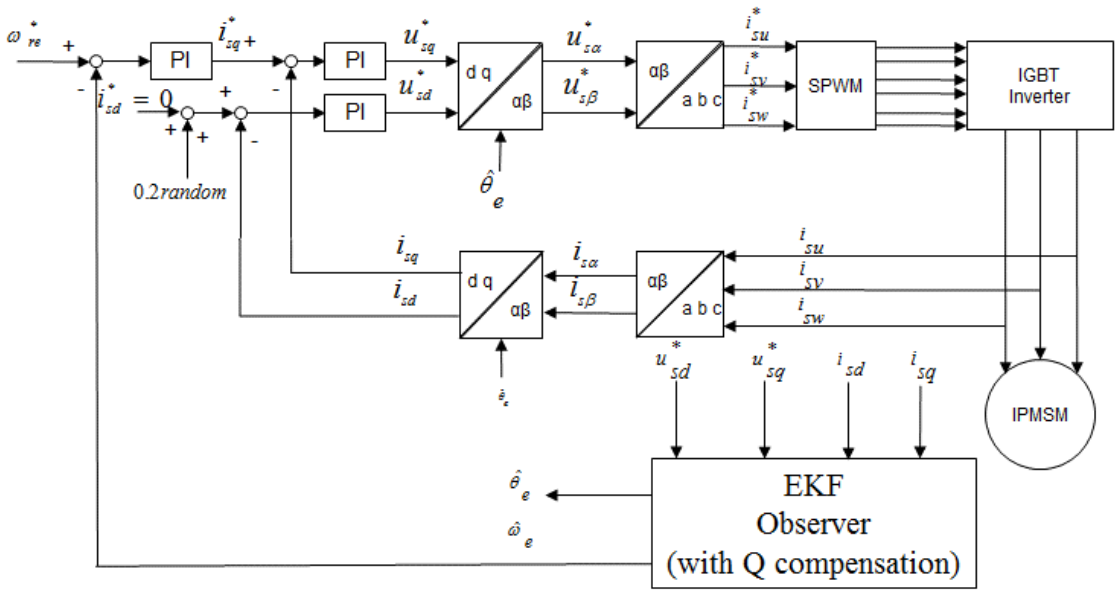

Fig.5.2 Simulation model III

(white random signal injection, with Q compensation)

(1). Model I is the normal EKF observer, no white random signal or Q compensation is added on system.

(2). Model II is the normal EKF observer, while white random signal is added on d-axis current command.

(3). Models III is the EKF observer with Q compensation, four terms in matrix Q of EKF, which is according to eq.(4.24), is compensated. At the same time, white random signal is added on d-axis current command.

Simulation is carried out by the three models above.

5.3 Simulation results

5.3.1 Simulation by model I

5.3.1.1 Simulation parameters by model I

Table III. EKF parameters for model I

P0_11	0.02
P0_22	0.02
P0_33	0.5
P0_44	0.0
Q11	0.15
Q22	0.15
Q33	4.0
Q44	0.0
Q13[0-1s]	0.0
Q13[1-5s]	0.0
Q14[0-1s]	0.0
Q14[1-5s]	0.0
R11	0.0001
R22	0.0001
White noise	0.0

5.3.1.2 Simulation results by model I

(1). 60rpm, without load torque situation

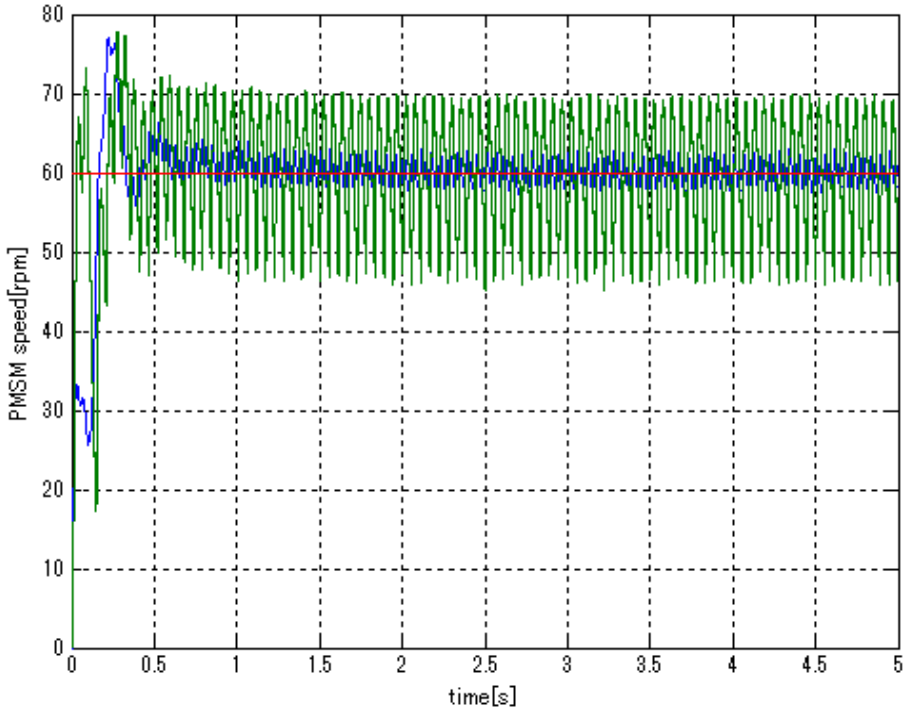

Fig.5.3 PMSM speed response at 60rpm command without load by model I

In Fig.5.3, the red line is the PMSM speed command. Green line is the speed signal from EKF observer, and the blue line is the measured speed signal.

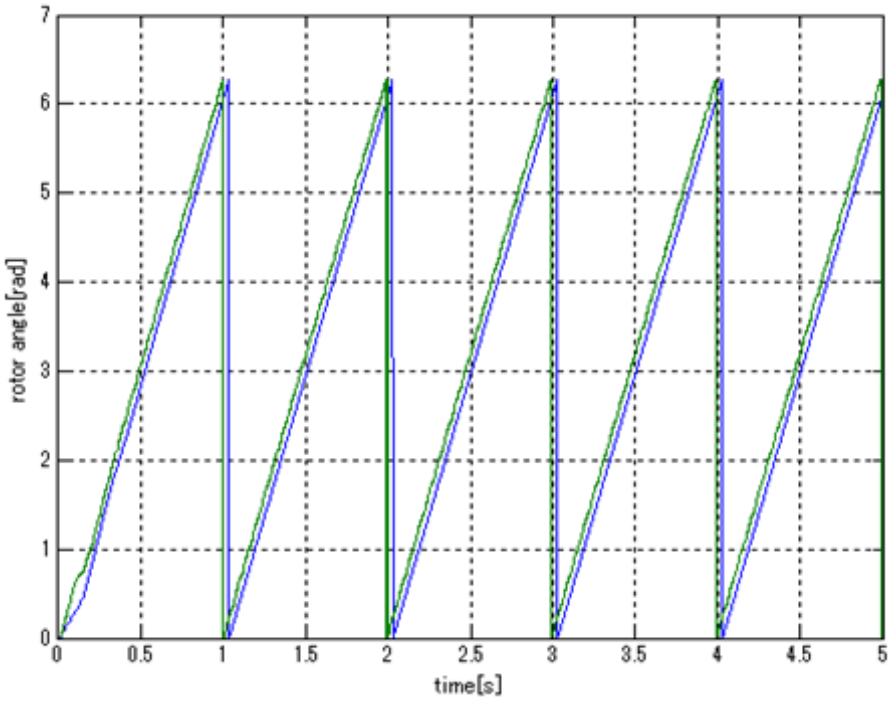

Fig.5.4 PMSM angle response at 60rpm command without load by model I

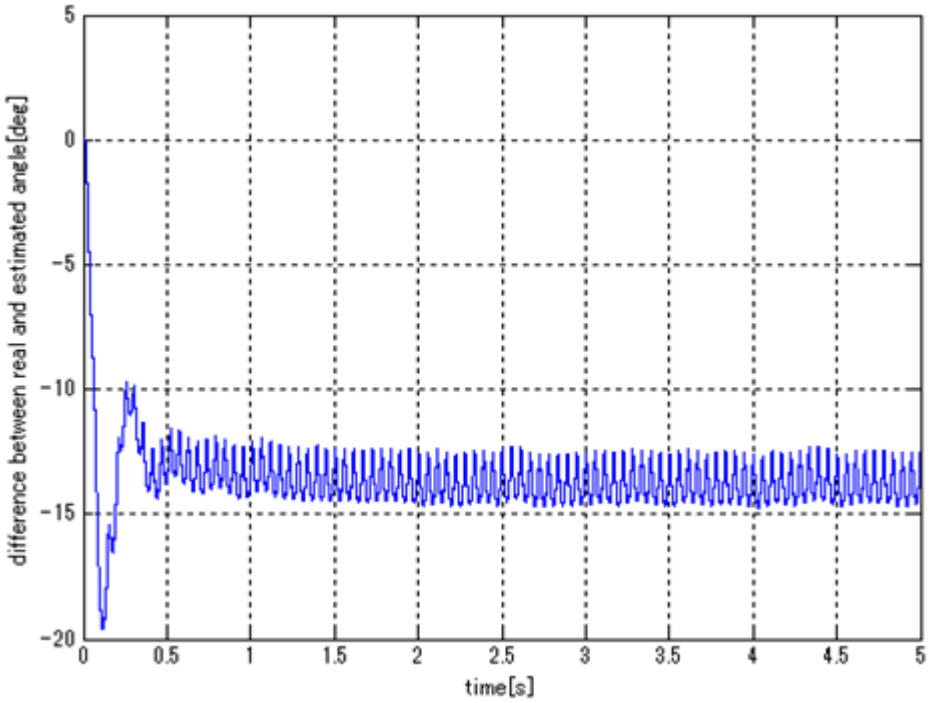

Fig.5.5 PMSM estimated and measured angle difference at 60rpm command without load by model I

(2). 60rpm, with load torque disturbance situation

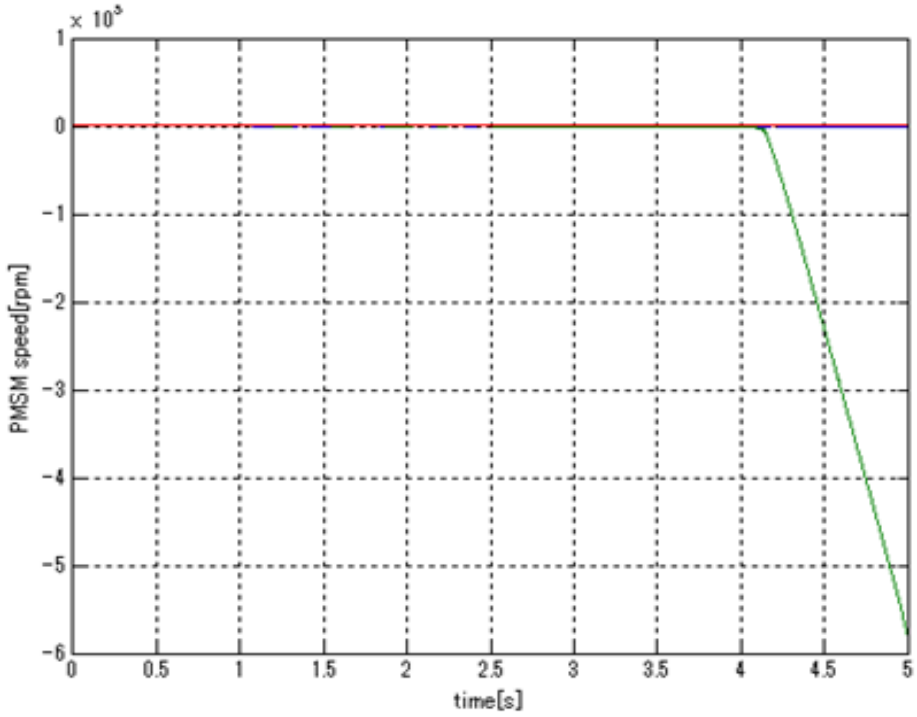

Fig.5.6 PMSM speed response at 60rpm command with load by model I

In Fig.5.6, it can be seen that when torque disturbance occurs, the estimated speed tends to infinite, while measured speed by encoder becomes 0.

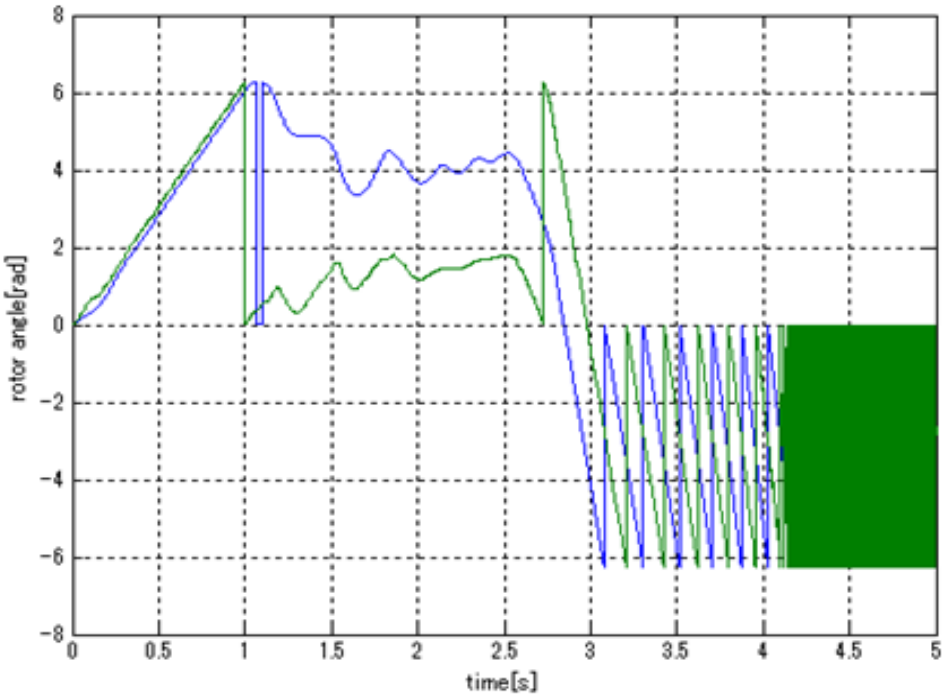

Fig.5.7 PMSM angle response at 0rpm command with load by model I

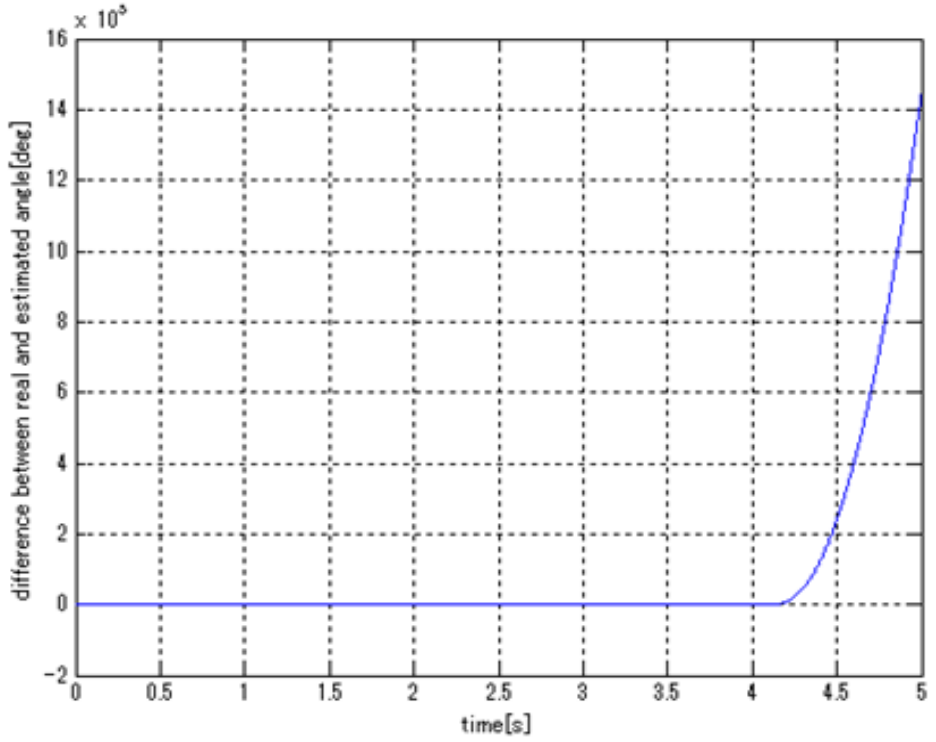

Fig.5.8 PMSM estimated and measured angle difference at 60rpm command with load by model I

(3). 0rpm, with load torque disturbance situation

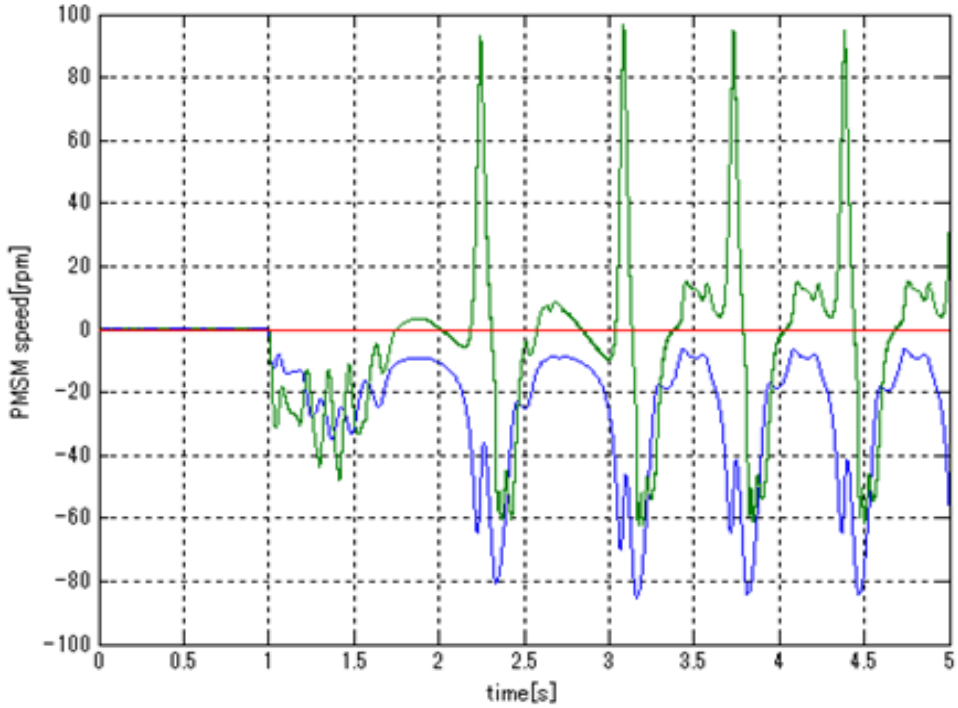

Fig.5.9 PMSM angle response at 0rpm command with load by model I

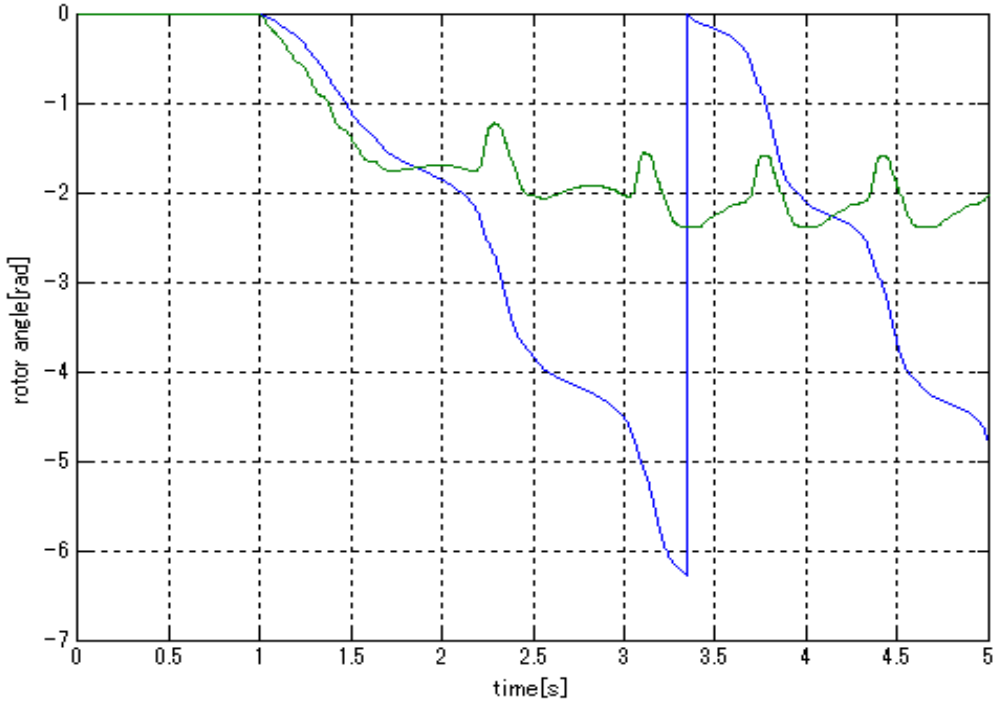

Fig.5.10 PMSM angle response at 0rpm command with load by model I

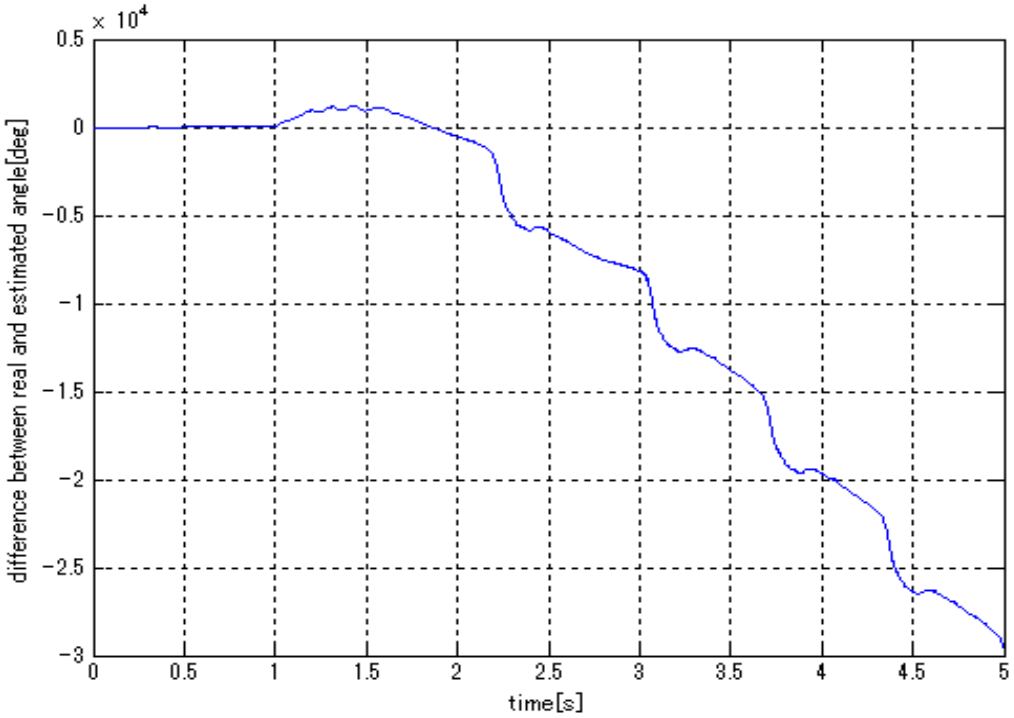

Fig.5.11 PMSM estimated and measured angle difference at 0rpm command with load by model I

5.3.2 Simulation by model II

5.3.2.1 Simulation parameters by model II

Table IV. EKF parameters for model II

P0_11	0.02
P0_22	0.02
P0_33	0.5
P0_44	0.0
Q11	0.15
Q22	0.15
Q33	4.0
Q44	0.0
Q13[0-1s]	0.0
Q13[1-5s]	0.0
Q14[0-1s]	0.0
Q14[1-5s]	0.0
R11	0.0001
R22	0.0001
White noise	0.2*random

5.3.2.2 Simulation results by model II

(2). 60rpm, with load torque disturbance situation

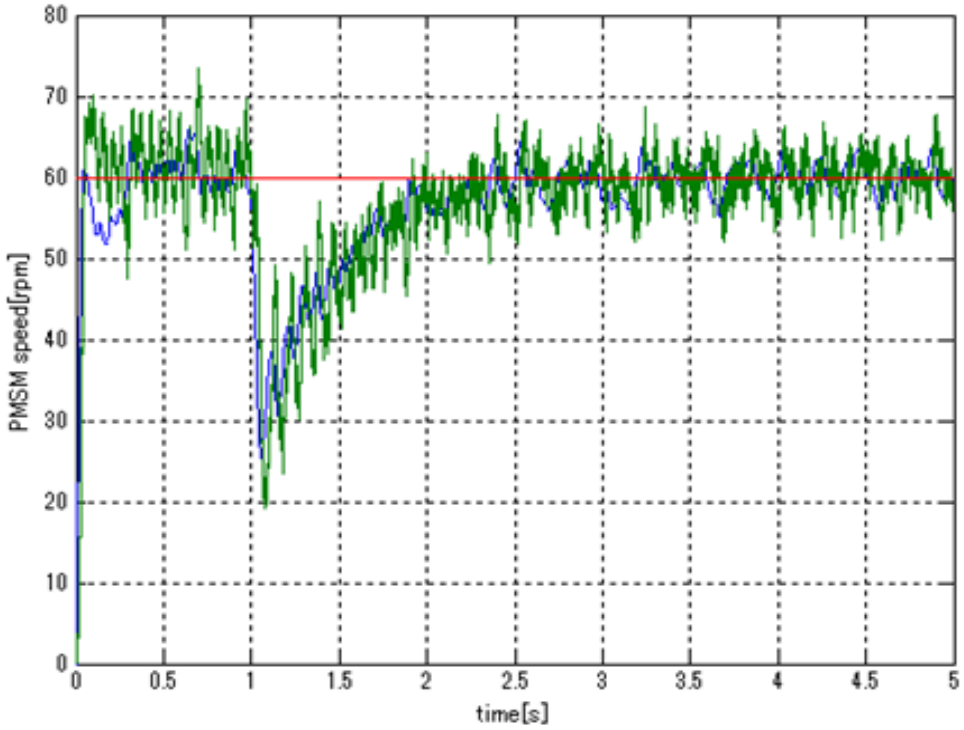

Fig.5.12 PMSM speed response at 60rpm command with load by model II

In Fig.5.12, the red line is the PMSM speed command. Green line is the speed signal from EKF observer, and the blue line is the measured speed signal. It can be seen that with white random noise injection, system can be controlled, compared to the same situation in model I.

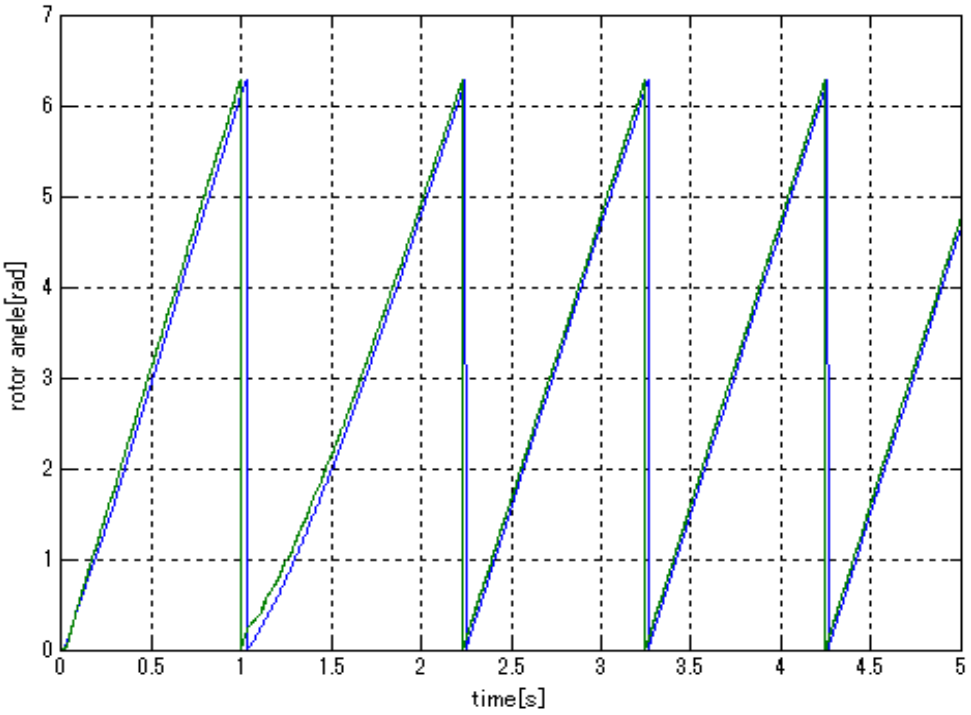

Fig.5.13 PMSM angle response at 60rpm command with load by model II

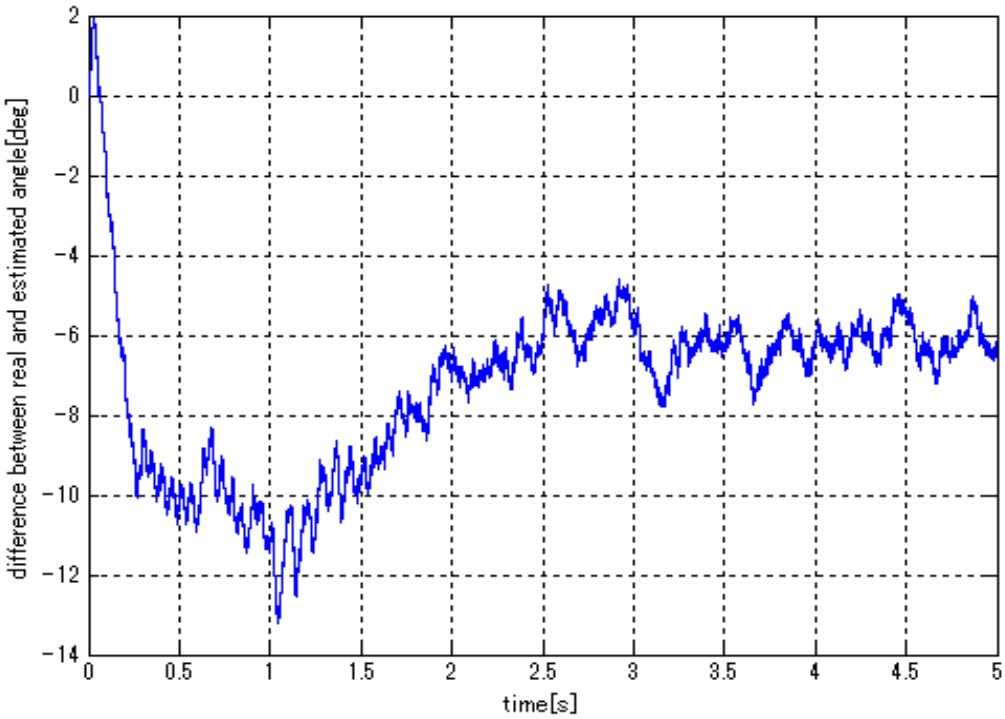

Fig.5.14 PMSM estimated and measured angle difference at 60rpm command with load by model II

(2). 0rpm, with load torque disturbance situation

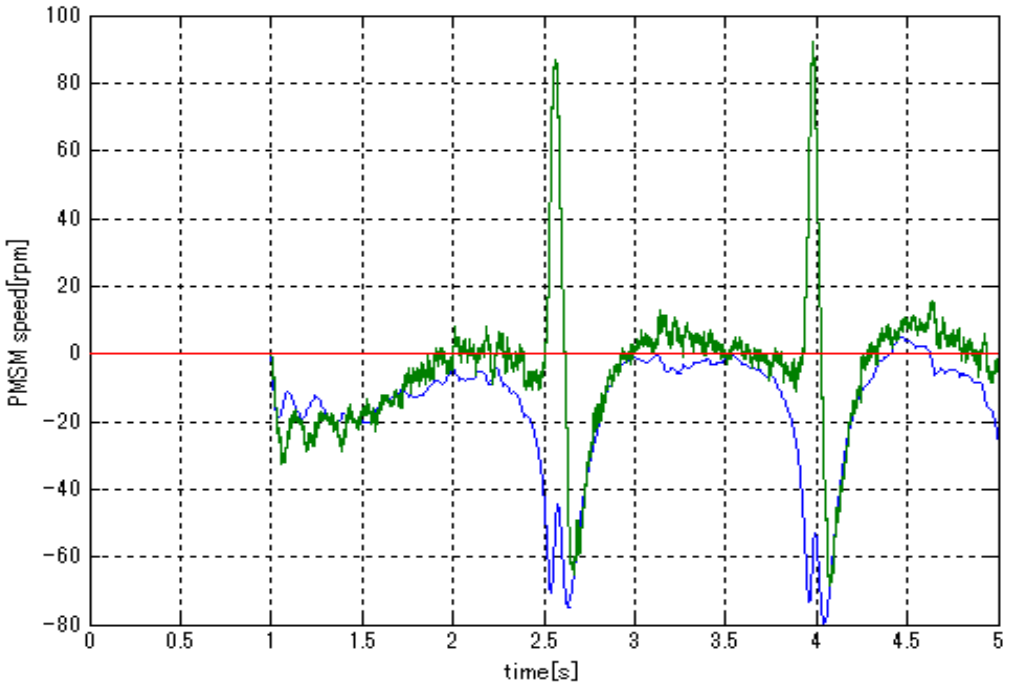

Fig.5.15 PMSM speed response at 0rpm command with load by model II

In Fig.5.15, the red line is the PMSM speed command. Green line is the speed signal from EKF observer, and the blue line is the measured speed signal from encoder. In 0rpm situation, PMSM cannot achieve position sensorless speed control with load torque.

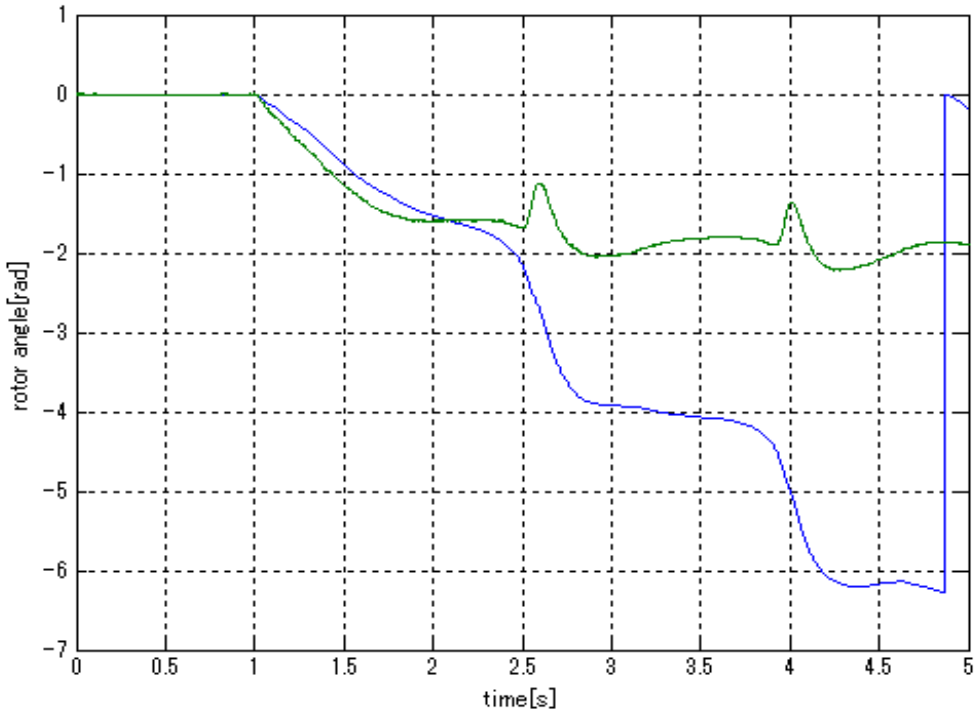

Fig.5.16 PMSM angle response at 0rpm command with load by model II

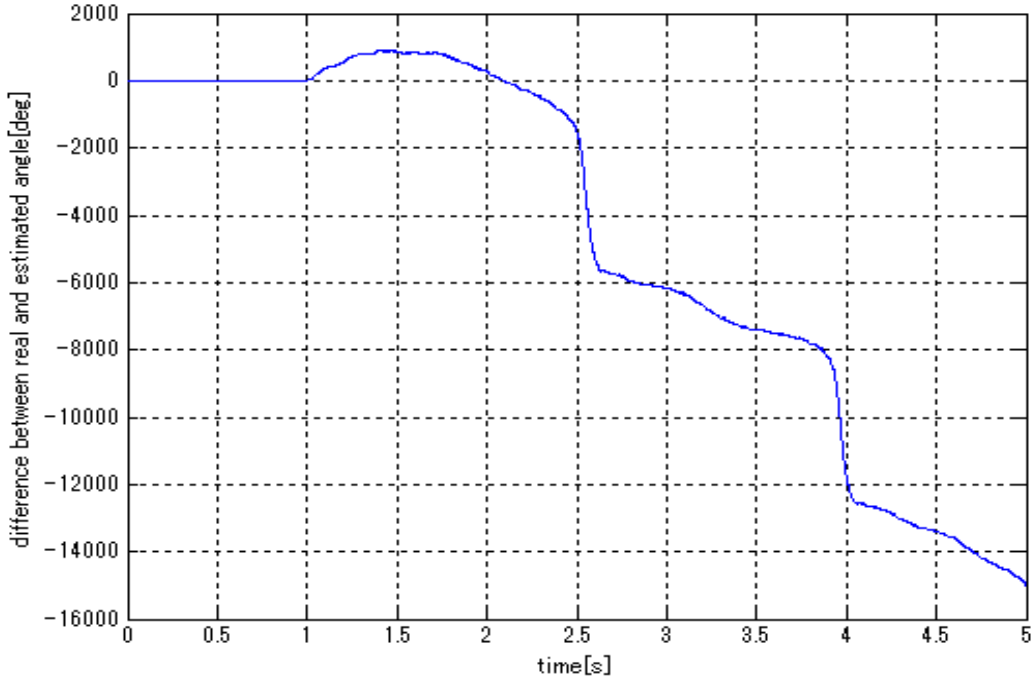

Fig.5.17 PMSM estimated and measured angle difference at 0rpm command with load by model II

5.3.3 Simulation by model III

5.3.3.1 Simulation parameters by model III

Table V. EKF parameters for model III

P0_11	0.02
P0_22	0.02
P0_33	0.5
P0_44	0.0
Q11	0.15
Q22	0.15
Q33	4.0
Q44	0.0
Q13[0-1s]	root(100.0)
Q13[1-5s]	root(150.0)
Q14[0-1s]	root(3.5)
Q14[1-5s]	root(2.7)
R11	0.0001
R22	0.0001
White noise	0.2*random

5.3.3.2 Simulation results by model III

(1). 60rpm, with load torque disturbance situation

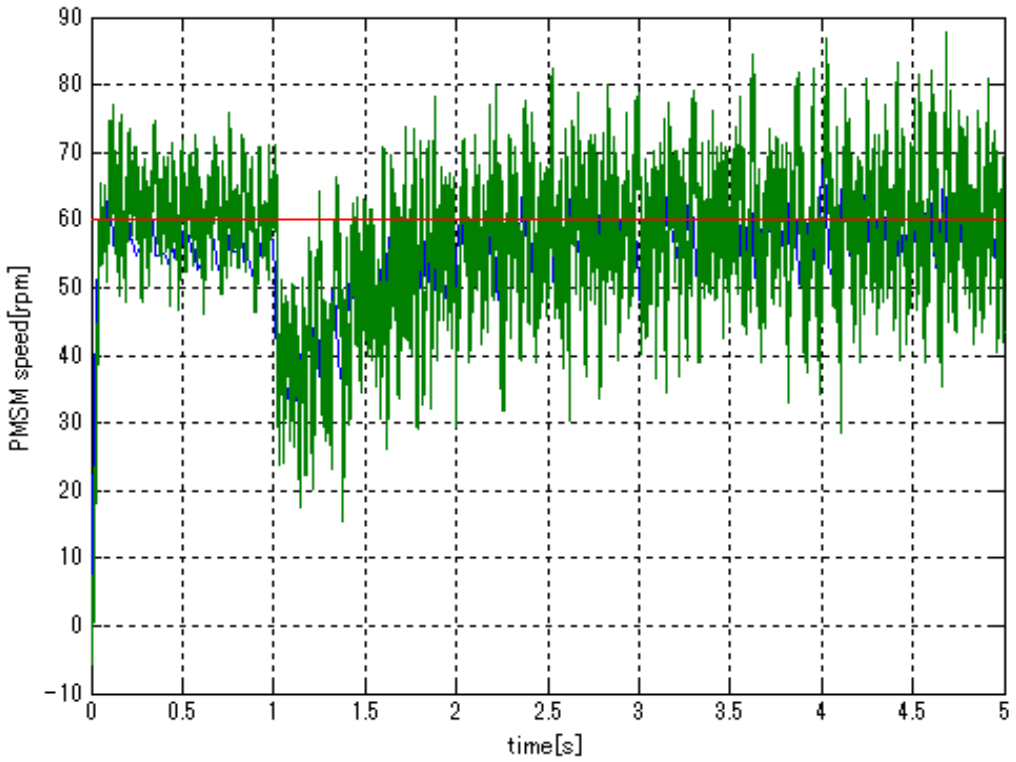

Fig.5.18 PMSM speed response at 60rpm command with load by model III

In Fig.5.18, the red line is the PMSM speed command. Green line is the speed signal from EKF observer, and the blue line is the measured speed signal. With Q compensation, system can achieve position sensorless speed control at low speed.

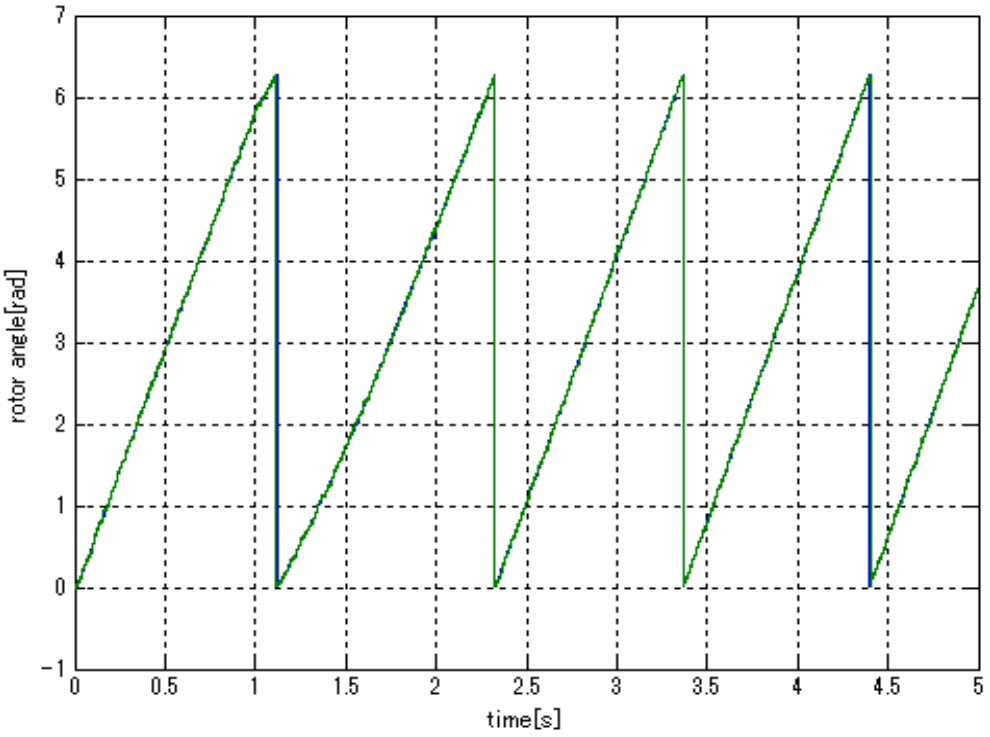

Fig.5.19 PMSM angle response at 60rpm command with load by model III

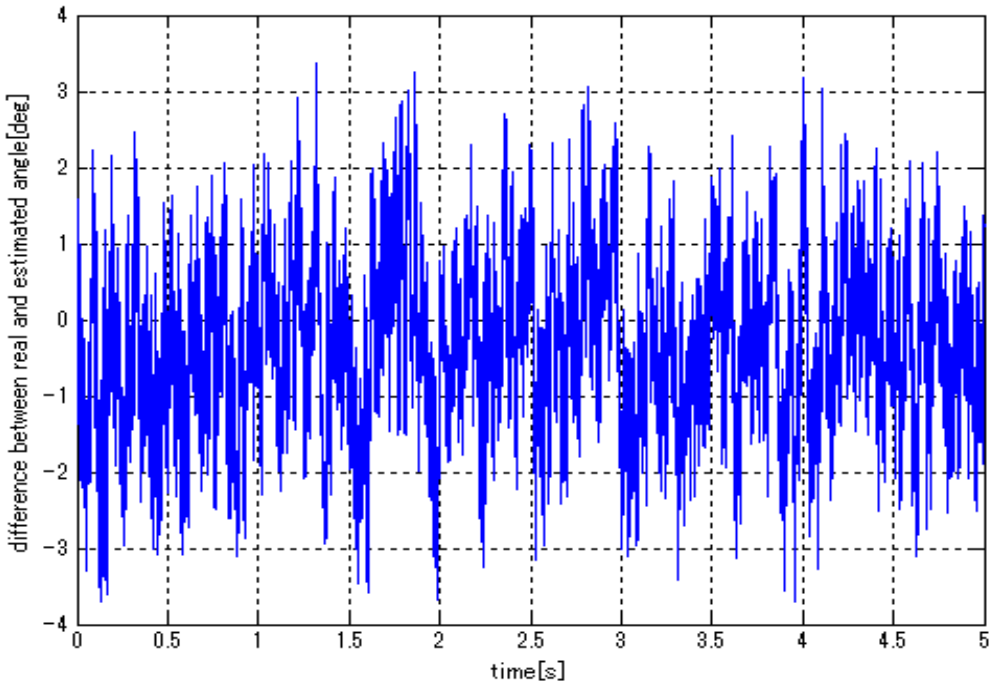

Fig.5.20 PMSM estimated and measured angle difference at 60rpm command with load by model III

(2). 0rpm, with load torque disturbance situation

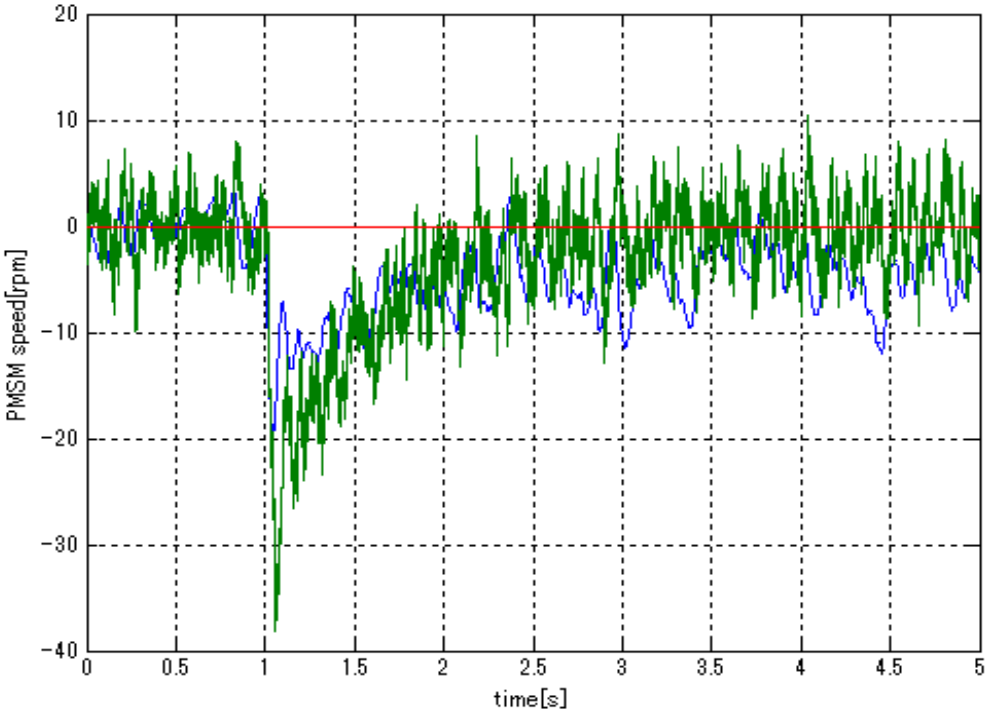

Fig.5.21 PMSM speed response at 0rpm command with load by model III

In Fig.5.21, the red line is the PMSM speed command. Green line is the speed signal from EKF observer, and the blue line is the measured speed signal. With Q compensation, system can achieve position sensorless speed control at 0 speed.

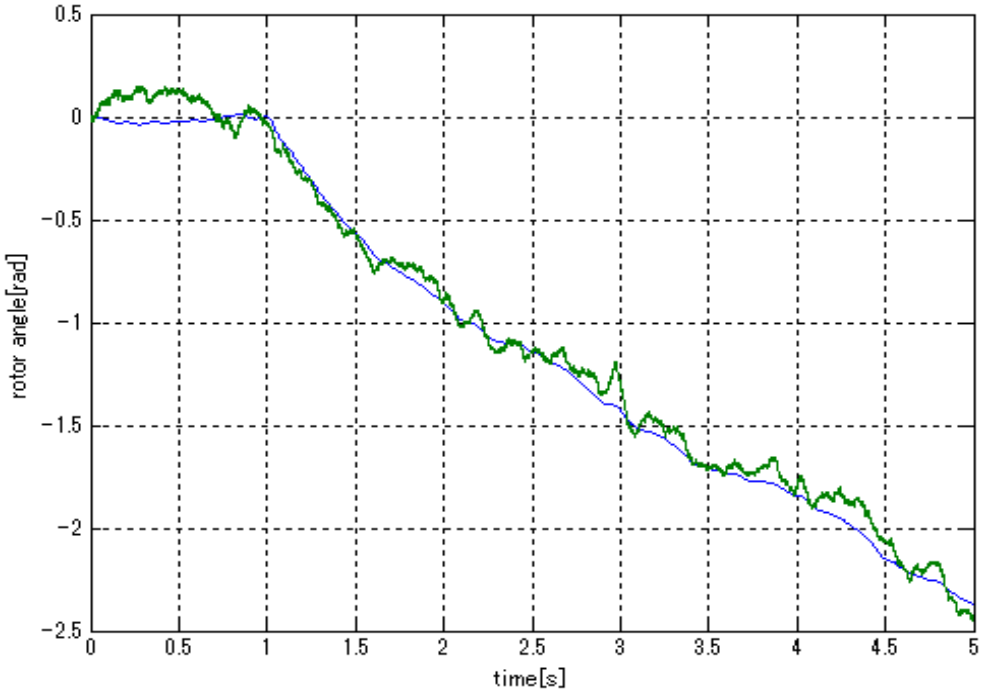

Fig.5.22 PMSM angle response at 0rpm command with load by model III

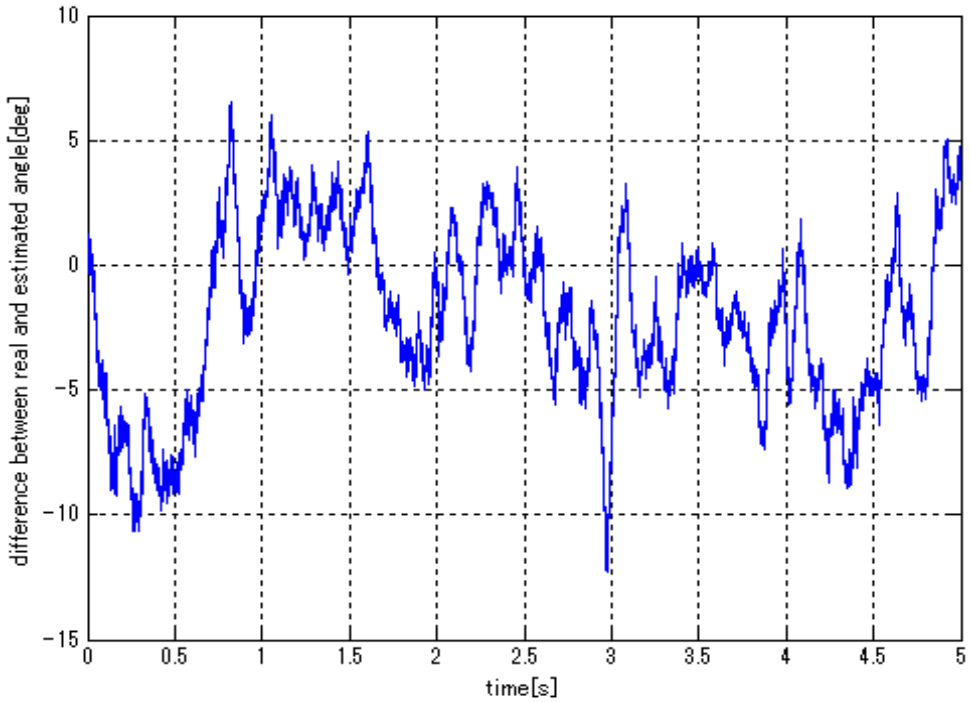

Fig.5.23 PMSM estimated and measured angle difference at 0rpm command with load by model III

5.4 Summary of simulation

Table VI. Comparison with torque situation in 60rpm command

60rpm	0[N*m]	0-0.5[N*m]	0-1[N*m]
Without white noise in id	Succeed	Fail	fail
With white noise in id	Succeed	Succeed	Fail
With white noise and Q compensation	Succeed	Succeed	Succeed

Table VII. Comparison with torque situation in 0rpm command

0rpm	0[N*m]	0-0.5[N*m]
Without white noise in id	Succeed	Fail
With white noise in id	Succeed	Fail
With white noise and Q compensation	Succeed	Succeed

In Table VI and VII, it is clear in 0-0.5[N*m] situation the system with white random noise in d-axis current command is better than the one without white random noise, while the system with white noise and Q compensation achieves the best performance. The reason why Q compensation can achieve better performance with load torque disturbance is shown in Fig.5.24.

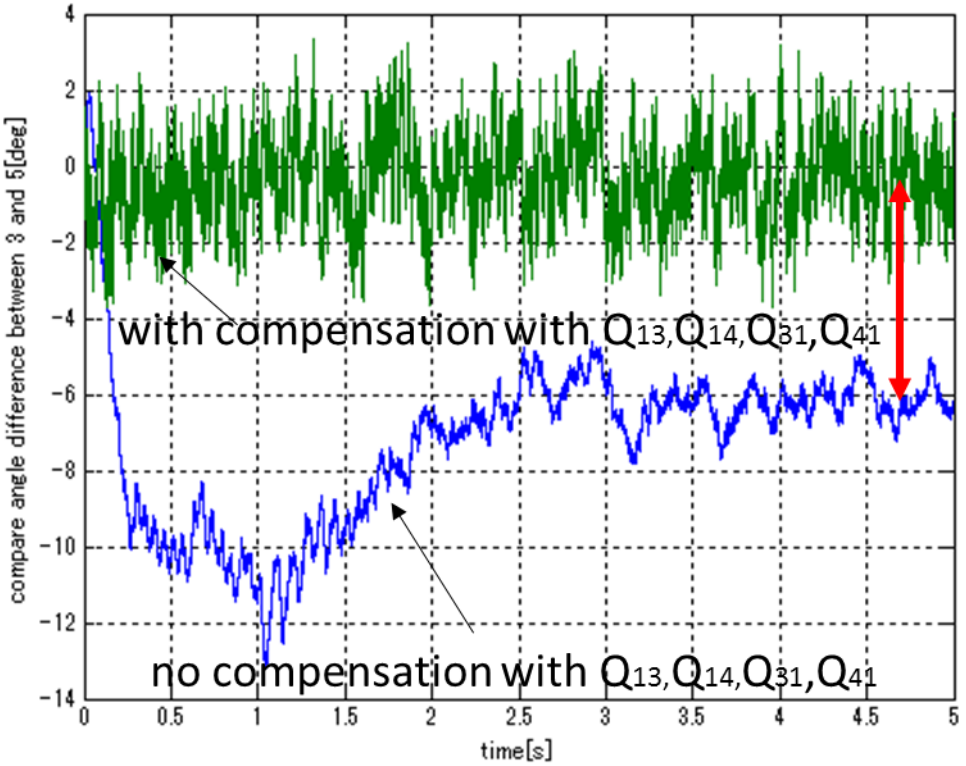

Fig.5.24 Comparison between Fig.5.14 and Fig.5.20

In Fig.5.24, blue line is the system angle difference with white random signal on d-axis current command only, and the green line is the system angle difference with not only white random signal but also Q compensation.

It can be seen that the green line has much smaller angle difference than the blue line. As in position sensorless sensorless control of PMSM, when load torque disturbance occurs, angle difference between estimated position and measured position will increase. It makes the whole system easier to be out of control. With proper Q compensation with reference to d-axis current can overcome this problem to some extend.

Chapter6. Conclusions and future works

6.1 Conclusions

In this research, a novel EKF PMSM position sensorless speed control system with d-axis white random current signal and nondiagonal matrix Q compensation is proposed.

Compared to the former research method, such as the system with EEMF Observer, novel EKF PMSM position sensorless speed control system can achieve PMSM low-speed position sensorless control, while system with EEMF Observer cannot(shown in Fig.6.1). The reasons why EEMF Observer cannot achieve low-speed range(defined as PMSM speed lower than 300rpm) control is:

(1). EEMF signals become complicated to be detected in low-speed range, as it is proportional to PMSM speed;

(2). There is low-pass filter in EEMF Observer, which aims at filtering the PMSM speed signal. Low-pass filter causes phase delay in motor position estimation. As a result, it is difficult to take load torque with EEMF Observer in low-speed range. At the same time, phase delay on speed estimation also causes the unstability of speed estimation.

Compared to the normal EKF PMSM position sensorless speed control system(shown in Fig.6.2), the novel one(shown in Fig.6.3) can not only achieve position sensorless control without load torque, but also the control with load torque.

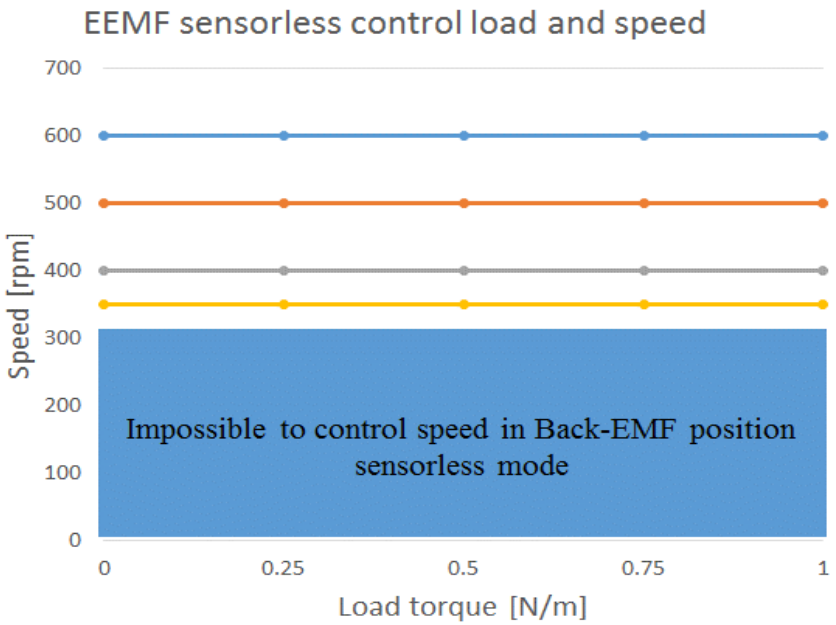

Fig.6.1 System load and speed relationships with EEMF observer

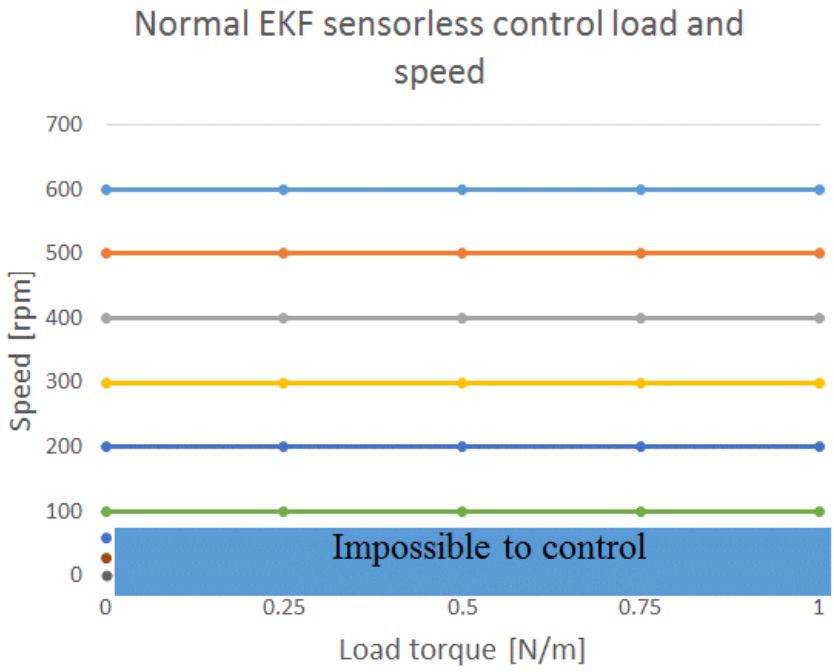

Fig.6.2 System load and speed relationships with normal EKF observer

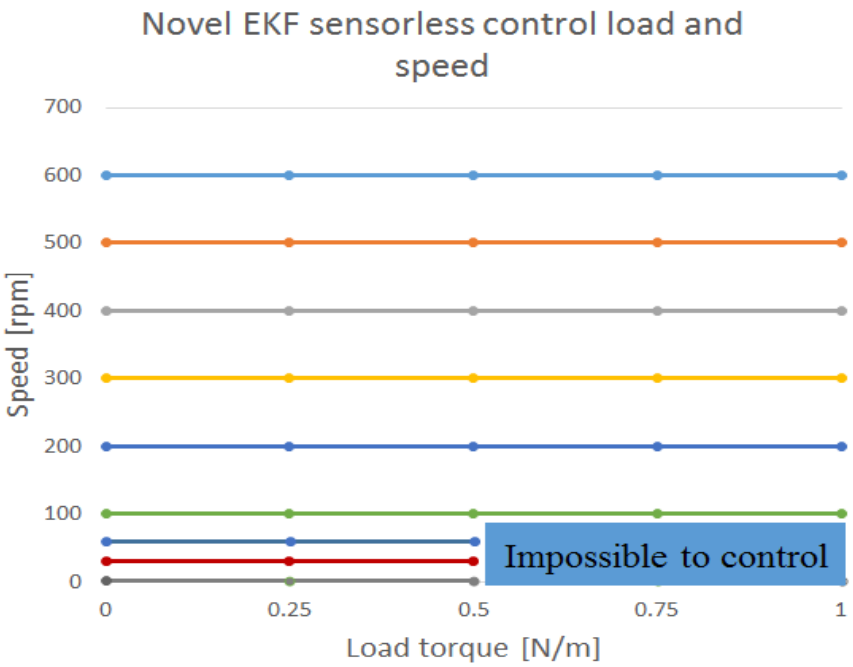

Fig.6.3 System load and speed relationships with novel EKF observer

6.2 Future works

Although this research has a little breakthrough in EKF low-speed range position sensorless speed control, there are still quite a lot works.

(1). The relationships between injected white random current signal with four novel compensation parameters in Q is studied by trial and error. There should be some mathematic logical relationships between them.

(2). In simulation results, novel EKF PMSM position sensorless speed control system has smaller angle difference between estimated one and measured one, but the random error in this angle difference is amplified, which should be pointed out is that it may decrease the life time of PMSM. A method to reduce such a kind of random error should be studied.

Reference

[1] Kelso J A S. Human Motor Behavior: An Introduction[J]. Human Motor Behavior An Introduction, 1982.

[2] Gewald J B, Luning S, Walraven K V. Motor vehicles and people in Africa: An introduction[J]. Critical Care Medicine, 2009, 43(12 Suppl 1):S-251.

[3] Matthew A.B. Baker, Richard M. Berry. An introduction to the physics of the bacterial flagellar motor: a nanoscale rotary electric motor[J]. Contemporary Physics, 2009, 50(6):617-632.

[4] Grush R. An introduction to the main principles of emulation: motor control, imagery, and perception[J]. Cognitive Psychology, 2002.

[5] Yang H, Jian Y, Bing X. Computational simulation and experimental research on speed control of VVVF hydraulic elevator[J]. Control Engineering Practice, 2004, 12(5):563-568.

[6] Khoucha F, Lagoun S M, Marouani K, et al. Hybrid cascaded H-bridge multilevel inverter motor drive DTC control for Electric Vehicles[C]// International Conference on Electrical Machines. IEEE, 2008:1-6.

[7] Wang X, Qin H, Li D. Research on the Four-Switch Three-Phase Inverter Fed PMSM-FOC System[M]// Electrical, Information Engineering and Mechatronics 2011. Springer London, 2012:1937-1944.

[8] Khadem R. foc control of PMSM using model predictive control[M]// Model predictive control /. Springer, 2004:309–329.

Reference

[9] Ke Z, Zhang X G, Li S, et al. Sliding mode control of high-speed PMSM based on precision linearization control[C]// International Conference on Electrical Machines and Systems. IEEE, 2011:1-4.

[10] Han Y S, Choi J S, Kim Y S. Sensorless PMSM drive with a sliding mode control based adaptive speed and stator resistance estimator[J]. IEEE Transactions on Magnetics, 2002, 36(5):3588-3591.

[11] Chi S, Zhang Z, Xu L. A Novel Sliding Mode Observer with Adaptive Feedback Gain for PMSM Sensorless Vector Control[C]// Power Electronics Specialists Conference, 2007. Pesc. IEEE, 2007:2579-2585.

[12] Zhu H, Xiao X, Li Y. A simplified high frequency injection method for PMSM sensorless control[C]// Power Electronics and Motion Control Conference, 2009. Ipemc '09. IEEE, International. IEEE, 2009:401-405.

[13] Calligaro S, Petrella R. Accuracy and robustness improvement in sensorless PMSM drives at low-speed by direct-axis current injection[C]// Sensorless Control for Electrical Drives. IEEE, 2013:1-5.

[14] 杉本, 小山, 玉井:「AC サーボシステムの理論と設計の実際」総合電子出版社, 1990.

[15] Z. Chen, M. Tomita, S. Doki and S. Okuma, "An Extended Electromotive Force Model for Sensorless Control of Interior Permanent-Magnet Synchronous Motors", IEEE Trans. IE, Vol.50, No.2, pp.288-295, 2003

[16] Xie C. Discuss on the PMSM Model of Power System Blockset in MATLAB5.3[J]. Electric Drive, 2003.

[17] Ilioudis V C, Margaris N I. Speed and position estimation technique for PMSM based on

modified machine model[C]// International Conference on Optimization of Electrical and Electronic Equipment. IEEE, 2010:407-415.

[18] Z. Chen, M. Tomita, S. Doki and S. Okuma, "An Extended Electromotive Force Model for Sensorless Control of Interior Permanent-Magnet Synchronous Motors", IEEE Trans. IE, Vol.50, No.2, pp.288-295, 2003

[19] Comanescu M. Rotor position estimation of PMSM by Sliding Mode EMF observer under improper speed[C]// IEEE International Symposium on Industrial Electronics. IEEE, 2010:1474-1478.

[20] Bedetti N, Calligaro S, Petrella R. A novel approach to the design of back-EMF observer based sensorless control of non-salient PMSM: Theoretical analysis and experimental investigations[C]// IEEE Energy Conversion Congress and Exposition. IEEE, 2013:3496-3503.

[21] Lerro D, Bar-Shalom Y. Tracking with debiased consistent converted measurements versus EKF[J]. Aerospace & Electronic Systems IEEE Transactions on, 1993, 29(3):1015-1022.

[22] Jiménez A R, Seco F, Prieto J C, et al. Indoor pedestrian navigation using an INS/EKF framework for yaw drift reduction and a foot-mounted IMU[C]// Positioning Navigation and Communication. IEEE, 2010:135-143.

[23] Ouhrouche M A. Estimation of speed, rotor flux, and rotor resistance in cage induction motor using the EKF algorithm[J]. International Journal of Power & Energy Systems, 2002, 22:103-109.

[24] Esteves F M, Nehmetallah G, Abot J L. Low-cost attitude determination system using an extended Kalman filter (EKF) algorithm[C]// SPIE Defense + Security. 2016:98421K.

[25] Wang H, Wang J, Qu L, et al. Simultaneous Localization and Mapping Based on Multilevel-EKF[J]. 2011:2254-2258.

Reference

[26] Bailey T, Nieto J, Guivant J, et al. Consistency of the EKF-SLAM Algorithm[C]// Ieee/rsj International Conference on Intelligent Robots and Systems. IEEE, 2006:3562-3568.

Paper or conference paper that published

[1] Suthep S, Wang Y, Yuuma I, et al. Frame anti-vibration control for sensorless IPMSM-driven applications[C]// Industrial Electronics Society, IECON 2016 -, Conference of the IEEE. IEEE, 2016:2802-2808.

[2] Suthep S, Wang Y, Ishida M, et al. Frame Vibration Suppression Method for Sensorless PMSM Drive Applications[J]. Journal of Power Electronics, 2016, 16(6):2182-2191.

Acknowledgments

First of all, I would like to express my utmost gratitude to Professor Muneaki Ishida, and Professor Junji Hirai of Electrical and Electronic Engineering Department, Engineering School, Mie University, for being my advisor and mentor. Thanks for their friendship and help throughout years I live and study in these three years.

I also thank assistant assistant Professor Naoki Yamamura, Doctor Masato Koyama and Doctor Daisuke Yashiro, for many nice and interesting discussions on my research project, and for many valuable and insightful comments which are quite helpful for improving my research.

Thanks for Professor Satoshi Komada and assistant Professor Kazuhiro Yubai for providing very useful knowledge on my research work and valuable suggestions on this research.

Thanks for Mr. Masaki Hoshino, Mr. Nagano Yuki, Mr. Yuma Itokawa and all members of my research group and the students in control system research room and energy research room.

Finally, I would like to thank my family for their endless love, support and encouragement.